SRI VENKATESWARA INTERNSHIP PROGRAM FOR RESEARCH IN ACADEMICS (SRI-VIPRA)

SRI-VIPRA

Project Report : SVPG-2505

"Identification, characterization and validation of novel natural ligands against Mycobacterial target proteins using molecular docking."

SRI-VIPRA

IQAC
Sri Venkateswara College
University of Delhi
Benito Juarez Road, Dhaula Kuan, New Delhi
New Delhi -110021

SRIVIPRA PROJECT 2025

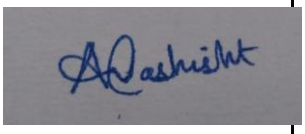
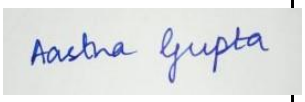
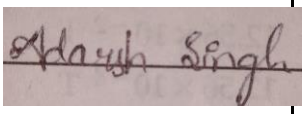
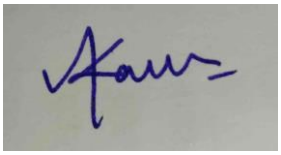
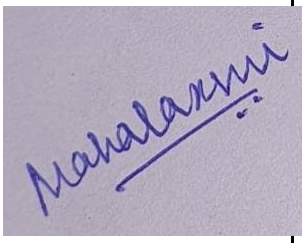
SVPG-2505

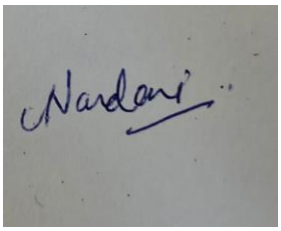
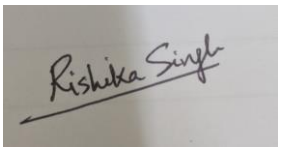
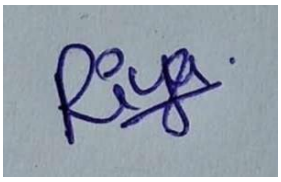
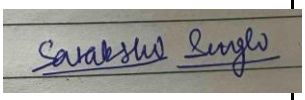
Title: "Identification, characterization and validation of novel natural ligands against Mycobacterial target proteins using molecular docking."

Name of Mentor: Dr Nimisha Sinha
Co-supervisor: Dr Vandana Malhotra
Name of Department: Biochemistry
Designation: Assistant Professor

Nimisha

Signature of Mentor

S. No.	Name of the student	Photo	Roll No.	Course	Signature
1	Aarav Vashisht		1223017	BSc (H) Biochemistry Semester V	
2	Aastha Gupta		1223036	BSc (H) Biochemistry Semester V	
3	Adarsh Singh		1323066	BSc (H) Biological Sciences Semester V	
4	Arshdeep Kaur		1224014	BSc (H) Biochemistry Semester III	
5	Mahalaxmi		1223043	BSc (H) Biochemistry Semester V	

6	Nandani Kumari		1323030	BSc (H) Biological Sciences Semester V	
7	Rishika Singh		1423055	BSc (H) Botany Semester V	
8	Riya		1123102	BSc Life Science Semester V	
9	Satakshi Singh		1223901	BSc (H) Biochemistry Semester V	
10	Sharanya Patnaik		1223059	BSc (H) Biochemistry Semester V	

Certificate of Originality

This is to certify that the aforementioned students from Sri Venkateswara College have participated in the summer project SVP-2505 titled ***"Identification, characterization and in vitro validation of novel natural ligands against Mycobacterial target proteins"***. The participants have carried out the research project work under my guidance and supervision from 1st July, 2025 to 31st December, 2025. The work carried out is original and carried out in an online/offline/hybrid mode.

Nimisha

Signature of Mentor

Acknowledgement

We first offer our heartfelt gratitude to the Almighty for the gift of health and perseverance throughout this journey. Our deepest thanks go to our families; their unwavering support and unconditional love have been our primary source of strength.

We are profoundly grateful to our mentors, ***Dr. Nimisha Sinha*** *and* ***Dr. Vandana Malhotra****, for their invaluable guidance and innovative insights. Their encouragement and open communication not only fueled our curiosity but significantly deepened our engagement with this work. It has been a distinct privilege to learn under their mentorship.*

We are also deeply thankful to everyone who contributed to the project, offering their assistance and correcting our mistakes along the way. Their support was crucial in completing the project within the designated time frame.

Finally, we thank our college for providing the resources and the academic environment that made this unforgettable experience possible.

TABLE OF CONTENTS

S.No	Topic	Page No.
1.	Abstract	8
2.	Introduction/Background	9-15
3.	Materials/Methods	15-19
4.	Results	19-56
5.	Discussion	56
6.	References	57-59
7.	Utilization Certificate	60

Abstract

Tuberculosis persists as one of the world's leading public health crises till date. Historically, disease treatment has involved an amalgamation of first line and second line drugs that the causative microbe - *Mycobacterium tuberculosis* has developed resistance against over time. One of the major contributors towards its drug tolerance comes from the MFS family protein EfpA, which acts as an efflux pump, resulting in the expulsion of treatment medication. This study aims to identify natural ligands derived from marine organisms and plant sources as potential inhibitors of EfpA using bioinformatics-based molecular docking.

In this study, the 3D structure of EfpA was obtained from the Protein Data Bank (PDB), after which it was prepared for molecular docking using AutoDock 4.2. The potential inhibitors docked against this protein were derived from a comprehensive ligand library of natural compounds constructed through an extensive review of literature. This list was composed of bioactive, antimicrobial molecules, that were docked site-specifically with certain amino acid residues of the protein that depicted interactions with EfpA inhibitor BRD8000.3. The top-ranked ligands were selected based on binding energy scores, after which interactions were assessed, including hydrogen bonding and hydrophobic interactions.

The docking findings uncovered promising candidates displaying high-affinity interactions with EfpA. Some of the ligands showed stable interactions within the critical site of the receptor protein, suggesting potential inhibitory effects on EfpA protein function. This study demonstrates the potential of certain natural compounds as novel inhibitors targeting EfpA, thus revolutionising the efficacy of the current treatment regimen. Future experimental validation is required to confirm these findings and elucidate the mechanisms of action.

Keywords: *Mycobacterium tuberculosis*, EfpA, efflux pumps, natural ligands, molecular docking, drug resistance

1. Introduction

1.1 Global Prevalence of Tuberculosis

Across all continents, infection with *Mycobacterium tuberculosis* is still one of the most commonly encountered bacterial infections. Of the world's population, one quarter is expected to be carrying latent tuberculosis infection, which equates to around 1.72 billion people. This latent pool is the main source of potential future active cases, however only a small percentage of infected persons actually develop illness during their lifetime (Cohen, A. et al. (2019)).

The worldwide latent *M. tuberculosis* infection prevalence is generally given as about 23-30% of the total population, but with major differences from one region to another.

To give a current example from worldwide TB cases, the annual number of newly diagnosed TB cases is estimated to be in the range of 1011 million, which calculates to an incidence of roughly 130140 cases per 100, 000 population per year.

It follows that the point prevalence of active TB at any moment in time that is, the number of individuals with clinically manifest disease is likely to be in the range of hundreds of thousands up to more than one million cases, with a very large proportion of the burden concentrated in highburden countries such as India, Indonesia, China, the Philippines, Pakistan, Nigeria, and Bangladesh. This data clearly highlight the continued prevalence of tuberculosis (Houben, R. M. G. J., & Dodd, P. J. (2016)).

1.2.1 Life cycle and pathogenesis

Mycobacterium tuberculosis is spread by the aerosolized droplets expelled by the infected individuals. These bacteria, when inhaled, are taken up by the macrophages of the alveolar spaces in the lungs. Mycobacterium tuberculosis has developed many strategies for its survival and replication inside the host’s macrophages. They inhibit phagosome-lysosome fusion, damaging the host’s antimicrobial defenses, playing a major role in the pathogenicity. The pathogen has a mycolic acid cell wall, providing resistance against immune response, aiding chronic inflammation and tissue damage. The infection spreads, damaging the lungs, leading to intense coughing, which spreads the bacteria further, completing its life cycle.(Smith, 2003)

The immune system recruits macrophages, monocytes, and lymphocytes to the infectious sites, which results in the formation of granulomas to contain the infection, which is the main feature of tuberculosis pathogenesis. Inside the granulomas, the bacilli are met with low oxygen, nutrient scarcity, and immune pressure conditions which result in bacterial adaptation and long-term persistence. This ability to survive under hostile conditions enables it to survive long-term within the host.(Miggiano et al., 2020)

Granulomas provide active microenvironments which are influenced by the ongoing interactions between the host and the pathogen. Inside the granulomas *Mycobacterium tuberculosis* alters the host immune responses in a way that it prevents complete eradication while also taking care not to trigger excessive immune activation, which could endanger its own survival. These capabilities allow the bacteria to exist in a metabolically adapted and non -replicating state, which leads to a latent stage of tuberculosis. This loss of immune control leads to rupture of granulomas, which causes the bacteria to reactivate. This shows the dual nature of the granulomas in supporting the host's immune system while also aiding in the survival of the pathogen.(Warner et al., 2025)

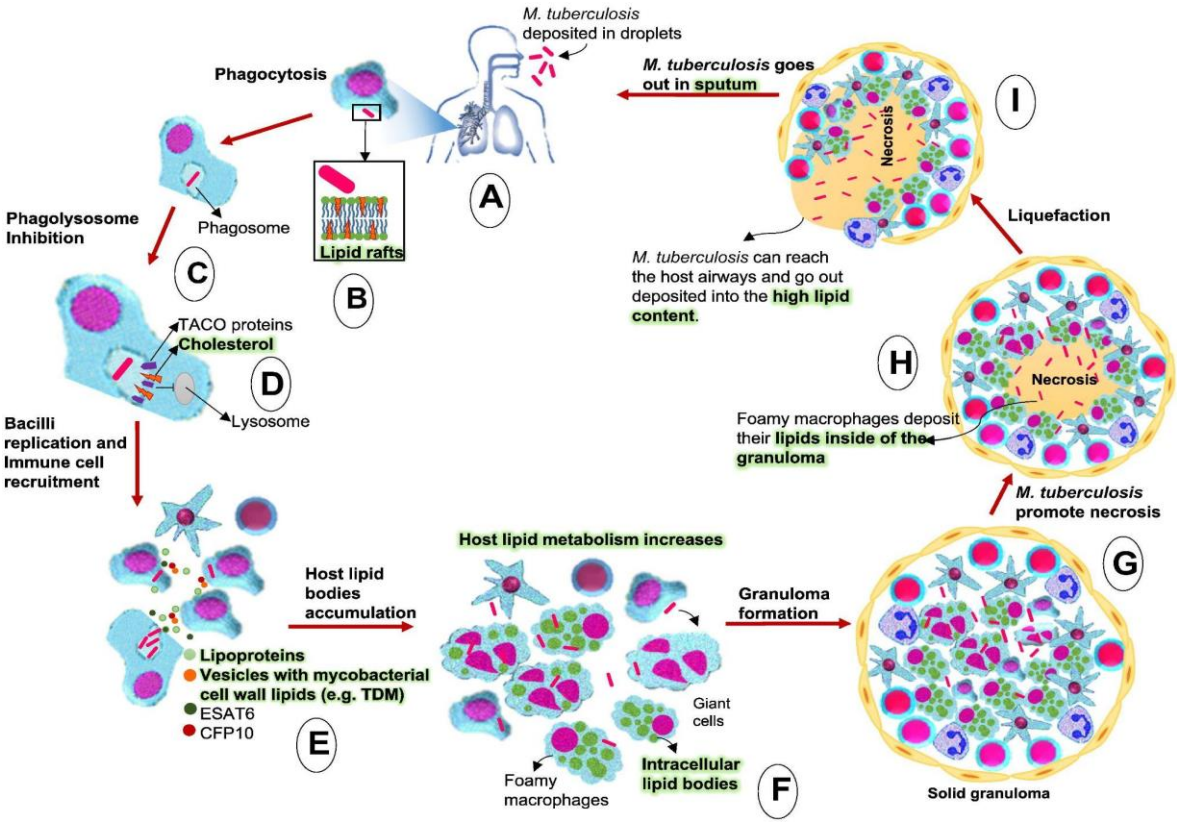


Figure-1: Systematic representation of life cycle of *Mycobacterium tuberculosis* in the host cells (Aguilar-Ayala et al., 2017).

Secreted proteins such as ESAT-6 and CFP-10 are specific for intensifying the pathogenicity of M. tuberculosis. These play a role in immune modulation and cause tissue damage, as they disrupt the host's cell membranes, after cytokine signaling pathways, promoting bacterial survival and spread. The reactivation of latent infection can lead to significant growth of bacteria, caseous necrosis, and cavitation of lung tissue, which leads to active disease and transmission to a new host. These mechanisms encapsulate

the complex life cycle and pathogenic strategies adapted by *M. tuberculosis*, ensuring its long-term survival and propagation in the human population.(Smith, 2003)

1.2.2 Signs and Symptoms

Mycobacterium tuberculosis (MTB) is the etiological agent of tuberculosis (TB), a chronic infectious disease affecting multiple organ systems. MTB infection may exist in two clinical states: latent tuberculosis infection and active tuberculosis disease. Latent MTB infection remains asymptomatic, with no observable clinical manifestations, despite immunological evidence of infection, due to effective containment of the bacilli by host immune mechanisms (Lawn SD et Zumla Al).

Active tuberculosis develops when the immune system fails to restrict bacterial replication, leading to clinical disease. The signs and symptoms of active MTB infection vary depending on the severity of infection and the anatomical site involved. Pulmonary tuberculosis, the most common form, primarily presents with respiratory manifestations. A persistent cough lasting three weeks or longer is the most frequently reported symptom, often accompanied by sputum production and, in advanced cases, hemoptysis (coughing up blood). Additional pulmonary symptoms include chest pain and dyspnea (shortness of breath), resulting from lung parenchymal and pleural involvement (Furin J et Cox H).

In addition to respiratory symptoms, active TB is characterized by prominent constitutional or systemic symptoms. These include prolonged fever, typically low-grade; night sweats; unintentional weight loss; fatigue or generalized weakness; and loss of appetite. Clinical studies have consistently reported cough, weight loss, and fever as the most prevalent symptoms among patients with active pulmonary TB (Furin J et Cox H, Golden MP, Vikram HR).

MTB may also disseminate beyond the lungs, giving rise to extrapulmonary tuberculosis, which presents with organ-specific clinical features. Tuberculous lymphadenitis commonly manifests as firm, painless lymph node swelling. Central nervous system involvement, such as tuberculous meningitis, may present with persistent headache, confusion, or neurological deficits. Skeletal tuberculosis, particularly spinal involvement, can result in chronic back pain and vertebral deformities, while laryngeal tuberculosis may cause hoarseness of voice. These extrapulmonary manifestations reflect the systemic spread and pathogenic versatility of MTB (Golden MP, Vikram HR,Velayutham B, Nair D, Tripathy JP et Chadha SS).

1.3.1 Cell wall assembly in Mycobacterium

One of the most complex membranes in bacteria is the cell wall of *Mycobacterium tuberculosis*, which is the causative agent of tuberculosis. Three segments, namely the plasma membrane, cell wall core, and outermost layer, constitute the cell wall. (Grzegorzewicz et al., 2016)The plasma membrane provides structural integrity and support. The strongly cross- linked peptidoglycan layer (PG) that envelops the plasma membrane forms covalent compounds with arabinogalactan (AG).(Singh et al., 2018) In

Mycobacterium tuberculosis, a majority of the cell wall is made up of AG ends, which are esterified with high molecular weight fatty acid called mycolic acid. The strong hydrophobic property of mycolic acid provides the bacteria protection from hydrophilic antibiotics and oxidative damage (Singh et al., 2017).

1.3.2 Primary Line of Treatment for Tuberculosis

In the standard treatment for drug sensitive tuberculosis (DS-TB), a set of four primary drugs - isoniazid (INH), rifampicin (RIF), pyrazinamide (PZA), and ethambutol (EMB) are provided in a combination to maximise therapeutic efficacy. This is also aimed at reducing the emergence of drug resistance in the patient.(*Global Tuberculosis Report 2023*, 2023) To guarantee high rates of treatment effectiveness and cure, this four-drug combination should be given under directly observed therapy (DOT) for at least six months. In order to eradicate the latent bacteria, the therapy is divided into two phases: the first phase, which consists of giving the four medications indicated above for two months, and the continuing phase, which uses INH and RIF for the last four months.(Zumla et al., 2013)

- Isoniazid (INH) is a prodrug which gets activated by the action of catalase peroxidase G (KatG) from the mycobacterium. Upon activation, isoniazid forms a covalent adduct with the NAD adduct which inhibits the enoyl-acyl carrier protein reductase (InhA). InhA is a key enzyme in the synthesis of mycolic acids (MA).(Rawat et al., 2003) The hydrophobic characteristics and lack of permeability of the mycobacterial outer layer are primarily mediated by the mycolic acids.(Marrakchi et al., 2014)

- Rifampicin (RIF) is a bactericidal drug used for primary treatment in drug- sensitive tuberculosis. It binds to the β- subunit of bacterial RNA polymerase (RNA pol II) thereby inhibiting the initial stages of gene transcription. This inhibition prevents RNA synthesis and ultimately leads to rapid suppression of mycobacterial growth.

- Pyrazinamide (PZA) serves as an indispensable sterilizing drug for treatment of drug sensitive TB. After diffusing into tuberculous granulomas, PZA is converted into its active form, pyrazinoic acid (POA). This conversion is catalyzed by the mycobacterial enzyme pyrazinamidase (PZAse). The generated POA exhibits potent bactericidal activity, particularly against persistent bacilli residing within the acidic environment of granulomas.(Zhang & Mitchison, 2003)

- Ethambutol (EMB) is a bacteriostatic drug that inhibits mycobacterial cell wall synthesis. This drug targets three different arabinosylgalactotransferases EmbA, EmbB and EmbC, which are required for the synthesis of arabinogalactan and lipoarabinomannan - essential components of the cell wall. (Goude et al., 2009)

1.3.3 Current DS-TB Treatment and its consequences

For drug-susceptible TB, the World Health Organization (WHO) now recommends a six-month treatment regimen that is divided into an intense phase and a continuation phase.(*Global Tuberculosis Report 2023*, 2023) The rigorous phase, also known as HRZE, lasts for two months and involves the administration of isoniazid (H), rifampicin (R), pyrazinamide (Z), and ethambutol (E). A four-month extension phase using isoniazid and rifampicin (HR) follows this. This procedure is based on years of clinical research and empirical data, and it has proven effective in most patients.

Liver dysfunction, peripheral neuropathy, erythromelalgia, ocular toxicity, central nervous system (CNS) toxicity, gastrointestinal (GI) intolerance, and skin rash are among the negative side effects linked to this regimen, even though the four front-line anti-TB agents are effective against DS-TB.

1.4 Challenges faced against TB and the need for a novel approach

1.4.1 MDR-TB and Emergence of Second-Line Drugs in TB Treatment

Multidrug-resistant tuberculosis (MDR-TB) is a deadly disease caused by *Mycobacterium tuberculosis* that are resistant to at least isoniazid and rifampicin, caused by mutations in the rpoB and katG genes, the two powerful first-line anti-tuberculosis drugs. A high rate of inappropriate or incomplete treatment, poor patient adherence and wrong combination of medicines, along with weaknesses in the tuberculosis (TB) control programs, has caused the emergence of MDR-TB, as these factors provide selective pressure to M. tuberculosis. The global burden of MDR-TB has exposed the inadequacy of first-line anti-TB drugs, requiring the use of second-line agents to treat tuberculosis.

These second-line drugs are less effective, more toxic, and require longer treatment times. These are the second-line injectable agents amikacin, kanamycin, and capreomycin, the oral bacteriostatic agents ethionamide, cycloserine, and para-aminosalicylic acid (PAS), and fluoroquinolones (i.e. levofloxacin and moxifloxacin). The addition of these second-line agents was a major step forward in the treatment of MDR-TB, but the first regimens resulted in poor treatment success. Further, they included a high pill burden, prolonged therapy (18-24 months), and significant adverse drug reactions. These problems highlighted the need for the development of more effective, safer, and shorter treatment regimens for MDR-TB, resulting in the creation of new anti-TB drugs and improved combinations.

1.4.2 MDR-TB Treatment

In the past decade we have seen great evolution in the treatment of MDR-TB. In the past we saw very long individualized regimens based on drug susceptibility which could last up to 24 months, had moderate results and high toxicity. We also saw that common side effects which included ototoxicity, nephrotoxicity, neuro psych issues and gut issues which in turn led to wide scale treatment break off or failure. Recently we have

seen great improvement in the management of MDR-TB with the introduction of new and re-purposed anti tubercular drugs like bedaquiline, delamanid, pretomanid, linezolid, and clofazimine. These drugs have made possible all oral, shorter and more effective regimens.
The World Health Organization made a recommendation in 2022 concerning the first totally oral 6-month regimen currently resistant to treatment and multidrug resistant TB (MDR/RR-TB). The regimen includes Bedaquiline, Moxifloxacin, Linezolid and Pretomanid (the BPaLM regimen), and in cases where a fluoroquinolone cannot be used, the Bedaquiline, Pretomanid and Linezolid regimen (BPaL). Reports have shown that these newer treatment protocols have achieved a significantly higher success rate in the treatment of TB, high rates of adherence by the patients, and have achieved a decrease in mortality rates, and decrease in the incidence of severe side effects, in comparison to older treatment protocols. The predominant strategy in the treatment of Multi-drug resistant tuberculosis (MDR-TB) is the early and accurate diagnosis using molecular methods, customizing the treatment regimens or using standardized regimens in accordance with the resistance patterns, the active monitoring of the patients' safety with the drugs, and focused care towards the patients. Even with these advancements, the treatment of high resistant TB continues to be a significant challenge. Most of these challenges remain in high burden countries, where the need for newer treatment drugs is high.(Hamada et al., 2021)

1.4.3 Co-infection with Other Diseases and XDR-TB

It is known that Mycobacterium tuberculosis persists within the human pulmonary alveoli in the form of latent granuloma. These latent bacteria survive and thrive even after completion of ATT therapies and will reactivate the infection when the host immune response gets compromised or dysregulated. Also, co-infection with other lethal diseases lead to creation of a favorable environment that the Mtb can take the chance to reactivate the disease and as a result increase the severities and complication of the disease in clinical settings. Among these, HIV is the most challenging one that the co-infection of HIV and MTb was recognized as one of the biggest challenge in public health due to severe weakening of the host immune functions by both pathogens and concurrent treatments of TB and HIV are very complicated because there is no integrated treatment regimes available, more numbers of pills to be taken by the patients, overlapping toxicity of drugs and drugs-drugs interaction and as a result it reduces the treatment efficacies and as a result poor clinical outcomes were observed.

The newly occurred Covid-19 has significantly worsened the global burden of TB by co-infecting SARS-CoV-2 with MTb. Because, both SARS-CoV-2 and MTb mostly affect the respiratory system, resulting on severe clinical complications and as a result it increases the mortality rate in TB patients from 1.5 million in 2020 to 1.6 million in 2021 and also it has been found that co-infection with SARS-CoV-2 leads to loss of LTBI people' protection. And all these above cases suggest that co-infection with XDR-TB or other diseases can complicate the diagnosis and treatment process in TB patients. Therefore, there is a need for the development of novel drugs and diagnostic tools for the early detection and treatment of TB from XDR-TB and other severe diseases.(TB/COVID-19 Global Study Group, 2022)

1.4.4 The Need for a Novel Approach to Drug Development

Research into some new findings about the pathophysiology of Mycobacterium tuberculosis, such as binding to the alveolar sacs, immune system evasion, and other methods of absorbing nutrients and metal ions, has been spurred by the previously mentioned challenges, such as MDR-TB, XDR-TB, various co-infections, etc. Consequently, we identified a family of proteins known as PE/PPE proteins, which are present in multiple strains of *Mycobacterium* and may be responsible for these actions.

1.5 Efflux Proteins

The activation of efflux pumps is one of the major acquired antibiotic resistance mechanisms that can lead to the development of MDR pathogens (Webber & Piddock, 2003). Efflux pumps are transport proteins localized in the cytoplasmic membrane of cells that actively translocate the chemical across the membrane (Gaurav et al., 2023). Efflux pump systems, widespread in many organisms, including gram-positive and -negative bacteria and eukaryotes (Rodrigues et al., 2020), are involved in the regulation of the internal environment by extruding out the toxic substances.

There are five major families of efflux-pump proteins: the ATP binding cassette (ABC) superfamily, the major facilitator superfamily (MFS), the multidrug and toxic-compound extrusion (MATE) family, the small multidrug resistance (SMR) family and the resistance nodulation division (RND) family. Efflux pumps are classified on the basis of the number of components that the pump has (single or multiple), the number of transmembrane-spanning regions that the transporter protein has, the energy source that the pump uses and the types of substrate that the pump exports (Piddock, 2006).

Even though there are various types of efflux pumps, substrate redundancy exists among all classes of efflux pumps, such that one antibiotic can be exported by several different efflux pumps and a single efflux pump can export structurally and chemically diverse substrates. Efflux pumps reduce bacterial susceptibility to antibiotics, and are essential for survival under stress, making them promising targets for novel inhibitors. Combined with existing antibiotics, these inhibitors could restore effective treatment, by reversing the resistance imparted by efflux pumps. However, substrate redundancy in efflux pumps creates uncertainty about clinical success of efflux pump inhibitors. Identifying novel, broad-spectrum efflux pump inhibitors may help overcome this challenge.

2. Material and Methods

2.1 Selection of Efflux pump proteins

A preliminary approach was carried out by discovering and extensively reviewing various research papers which were based on the potential functions executed by the efflux pump proteins (Wang et al. 2024). After thorough consideration, EfpA (Rv2846c) was finally selected. EfpA, the first major facilitator superfamily (MFS) protein identified in Mycobacterium tuberculosis (Mtb), is an essential efflux pump implicated in resistance to multiple drugs (Li et al. 2024). Exposure of Mtb to antibiotics such as isoniazid, rifampicin,

ABC	Rv2477	OFX, STR
	Rv2686c-Rv2687c-Rv2688c	FQs
	Rv2965-Rv2937-Rv2938	CHL, EMB, ERY, FQs, RIF, STR, TET
	Rv3756	PZA
MFS	Rv0191	CHL, EtBr, methylene blue, PZA
	Rv0783	INH, RIF
	Rv0809	AZI-533 (pyrrole), AMK
	Rv1258c (Tap)	Aminoglycosides, AZI-533 (pyrrole), INH, OFX, PZA, RIF, STR, TET
	Rv1410c (P55)	INH, EMB, RIF, CFZ
	Rv1643	FQs
	Rv2333c (Stp)	SP, TET
	Rv2350c (JefA)	INH, EMB
	Rv2484c (EfpA)	INH, TET
	Rv3008	PZA
	Rv3728	INH, EMB
RND	Rv2920 (MmpL7)	INH
	Rv0676c-Rv0677c (MmpL5-MmpS5)	BDQ, CFZ, azoles
SMR	Rv3065 (Mmr)	INH, EMB, EtBr, TPP, CTAB

and ethionamide can induce the expression of EfpA. Consequently, these compounds are expelled from the cell through EfpA driven by the proton motive force (Machado et al. 2012). High density mutagenesis and

deep-sequencing studies revealed that EfpA is essential for Mtb growth in vitro, indicating that it may also efflux critical endogenous substrates (Sassetti et al. 2003, Griffin et al. 2011).

2.2 Cryo-EM Structure Validation (Literature Review)

(i) Structure and Potential Role

Recent studies have revealed the cryo-EM structures of EfpA in an outward open conformation. The cryo-EM map displayed a dimeric assembly with a total of 28 transmembrane segments (TMs) (Wang et al. 2024). Each monomer contains 14 transmembrane helices, with both termini located on the cytoplasmic side. A hinge domain, containing a long loop, two TMs (TMs 7-8), and an amphiphilic helix (AH), is flanked by the N-terminal domain (NTD) consisting of TMs 1-6 and the C-terminal domain (CTD) consisting of TMs 9-14.

In the cryo-EM map of dimeric EfpA, strong nonproteinous densities, exhibiting two or four elongated tails, were identified at three adjacent sites (sites A-C) within EfpA (Wang et al. 2024). After thorough study, it was concluded that the densities were lipids. The four-tail density linking two monomers is likely cardiolipin, and the other two lipids are likely glycerophospholipids. The three lipids are generally parallel, instead of perpendicular, to the membrane surface. A solvent-accessible pathway within EfpA was identified using the MOLEonline program (Pravada et al. 2018). The pathway consists of three openings oriented toward the periplasm, the inner and outer leaflets of the phospholipid bilayer and accommodates the sequential binding of three lipids, forming a “staircase”-shaped pathway.

(ii) Ligand Binding Site Identification

BRD-8000s, a series of EfpA-targeting mtb inhibitors, were recently identified through high-throughput chemical-genetic screening (Johnson et al. 2019). In the cryo-EM map, BRD-8000.3 fit into the density at lipid-binding site, and displaced the cardiolipin (Li et al. 2024). BRD-8000s compete with lipids for binding to EfpA, thus disrupting its native functions, ultimately leading to mycobacterial cell death.

The lipid-binding tunnel in EfpA, which extends from the inner to the outer leaflet of the membrane, along with inhibitors that target the cardiolipin binding-site, provide strong evidence that EfpA acts as a lipid transporter.

2.3 Ligand Library

For the creation of a ligand library, 87 natural compounds extracted from plants were primarily selected after extensive literature research. Secondary metabolites such as flavonoids and alkaloids have proven to be beneficial to the development of various medications, while a renewed interest in utilising marine compounds due to their established antimicrobial activity is seen. The library comprises the names of the ligands, their structures (obtained from PubChem [https://pubchem.ncbi.nlm.nih.gov/]), molecular weight

as well as details relevant to Lipinski Rule of 5, which was used as the preliminary basis for the screening of ligands.

2.4 Ligand Validation

A ligand can be considered as a drug if it follows Lipinski's Rule of 5 it states that the Hydrogen Bond Donors should be Less than 5, Hydrogen Bond acceptors should be less than 10, Molecular weight less than 500 KDa and Partition coefficient less than 5. The Canonical SMILES of various ligands were retrieved from Pubchem (https://pubchem.ncbi.nlm.nih.gov/) and determined whether they follow Lipinski's Rule, using SwissADME (http://www.swissadme.ch/). The ligands that adhered to Lipinski's Rule were advanced for further docking.

2.5 Molecular Docking

Molecular Docking is used to study the interactions between the ligand and protein of interest. Various ligands from plant derivatives were docked against EfpA (Rv2846c) cryo-EM structure. The Docking was carried out using the AutoDock tool (https://autodock.scripps.edu/).

(i) Conversion of files to .pdbqt Form

After ligand validation using Lipinski's Rule of 5, their structures were retrieved from Pubchem (https://pubchem.ncbi.nlm.nih.gov/) in the .sdf form and converted to .pdbqt form using Openbabel(https://www.cheminfo.org/Chemistry/Cheminformatics/FormatConverter/index.html). The Protein structure of EfpA was converted to .pdbqt form using AutoDock by removing the already docked ligand (cardiolipin molecule) from its .pdb structure procured from Protein Database followed by the removal of water molecules. Polar Hydrogens and Kolman charges were added and AD4 Type was assigned and the file was saved as .pdbqt format.

(ii) Site-Specific Docking

To perform site-specific docking for EfpA, the amino acids present in the active site of the EfpA protein were first selected and the Grid box was placed such that it covers the active site region of the protein only by adjusting x, y and z coordinates. The grid box was saved as a .txt file, after which the file was saved in .gpf format. After this, the Autogrid command was executed in order to generate a .glg file, which provided us with the energy between receptor and ligand. After the creation of this file, now the Docking function was run wherein the Ligand file was selected, and the protein file was set as Rigid filename. Furthermore, under the header Searching Parameters, Genetic Algorithms was selected for docking that performs 10 runs, after which the file was saved in .dpf format. Finally, the Autodock command was executed to successfully generate the .dlg file.

2.6 Docking Analysis

The ligands that have lowest docking scores were determined using the RMSD table from the .dlg file. Their interactions and binding energies were examined and the file was saved as .pdbqt format. Further evaluation of interactions were performed on Discovery Studio Visualiser (https://discover.3ds.com/discovery-studio-visualizer-download) and a 2D diagram was generated exhibiting Protein-Ligand interactions.

3. Results

3.1 Active site of EfpA as per its Cryo-EM structure

The active site of efflux pump protein EfpA was characterised by a set of amino acid residues: Y97, S155, S69, T66, Q62, S191, Q443 and S444 [28]. Firstly, the B chain of EfpA was removed for ease of analysis. For site-specific docking, the mentioned amino acids were selected under A chain, and the dimensions of the grid box were set accordingly such that all of these residues were covered.

According to latest research the structural features of MtEfpA indicate that its central hydrophilic cavity functions not only as a substrate-binding site but also as a promising pocket for inhibitor binding. This cavity measures roughly 6–10 Å in width and contains a negatively charged inner surface lined by residues Y97, S155, S69, T66, Q62, S191, Q443, and S444. Its size, charge distribution, and orientation align well with the physicochemical properties of hydrophilic substrates such as EtBr and INH, suggesting that molecules with similar features could effectively bind and block this site. The conserved residue Y97, which is solvent-exposed and faces the periplasm, may play a critical role in stabilizing such interactions. These characteristics collectively highlight the central cavity as a credible and structurally well-defined site for designing inhibitors that target EfpA function.

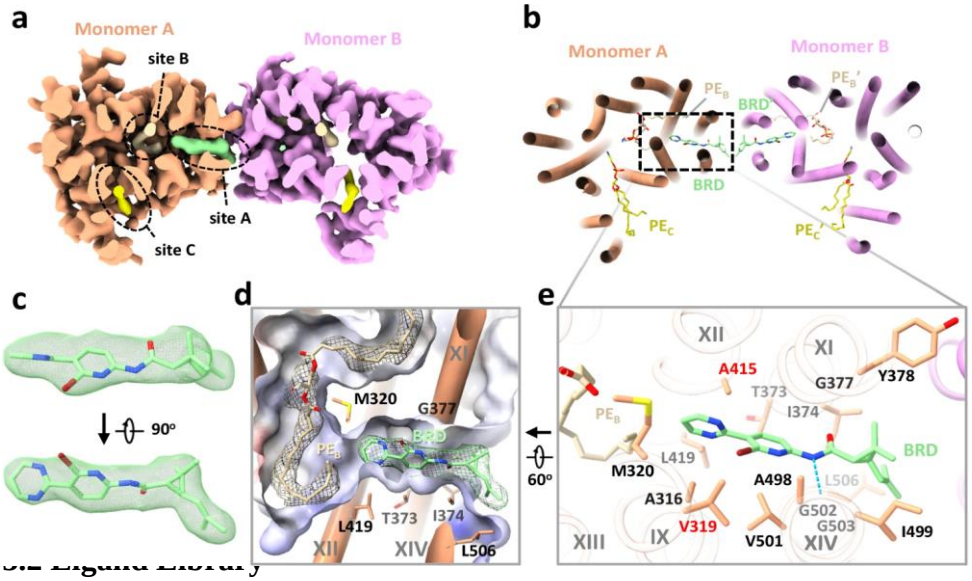
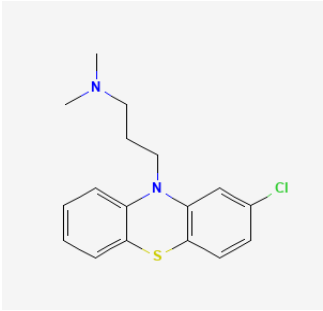
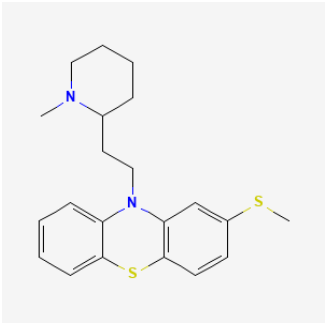
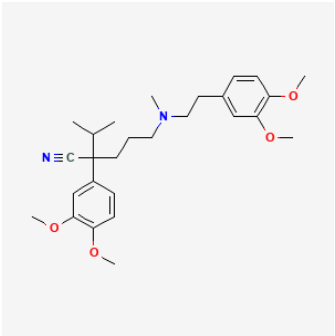
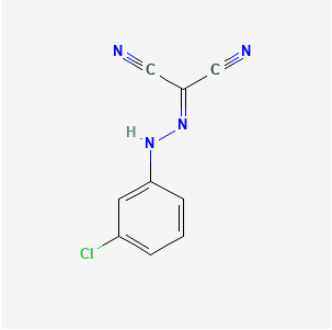
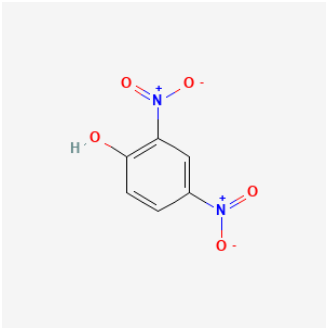
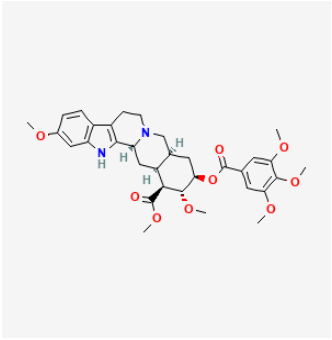


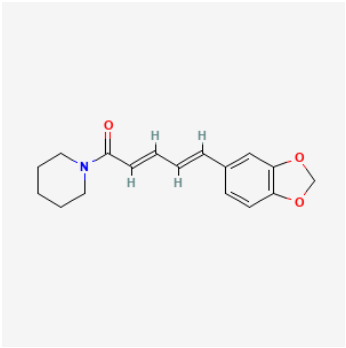
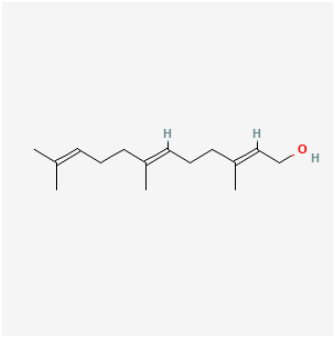
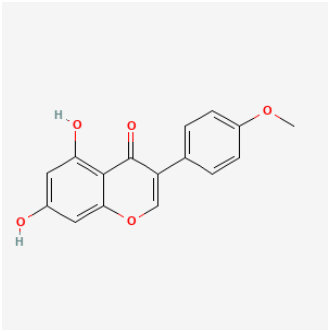
Figure 2: The interacting amino acid residues present in the active site of EfpA

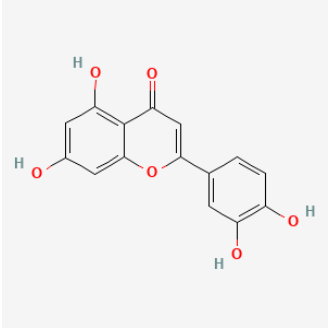
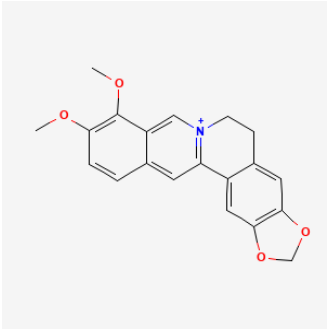
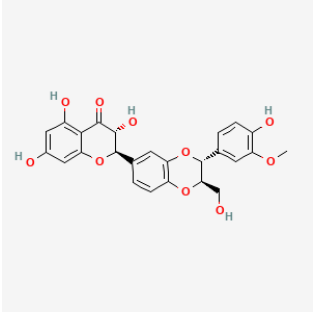
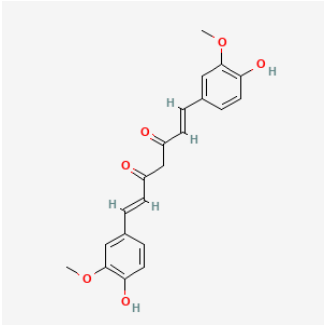
These are the list of ligands that were selected through literature review. The ligands have potential antimicrobial activity; these ligands are obtained from plant-derived sources like flavonoids and alkaloids. Some of the ligands have played an important role in inhibiting the efflux pump and help in increasing the efficiency of the antimicrobial ligands.

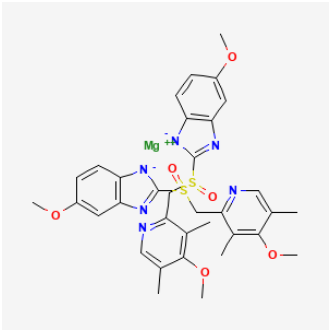
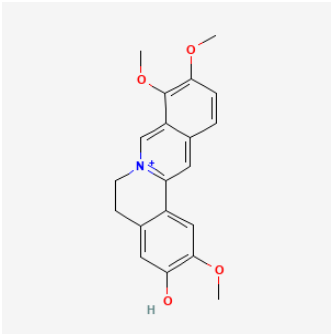
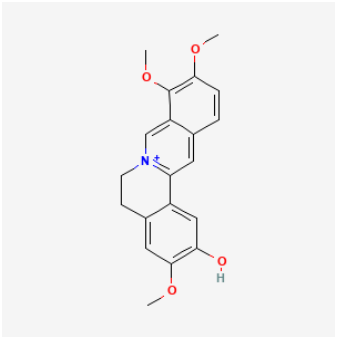
Table 2. Compilation of all ligands used with their Lipinski validation data

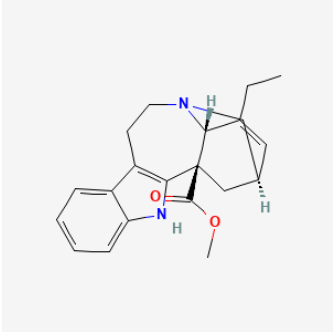
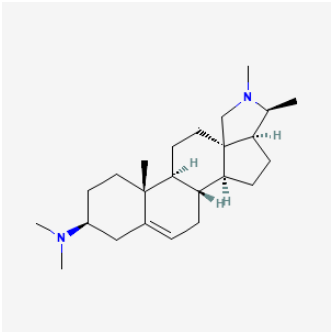
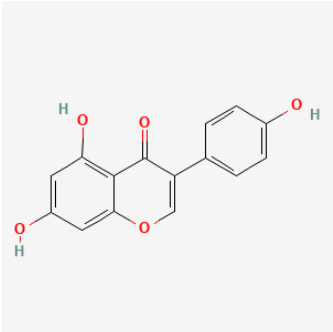
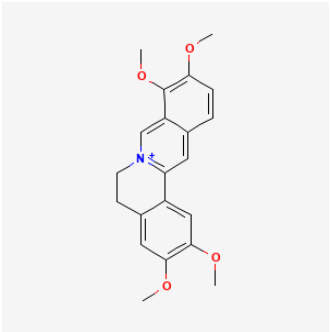
S. No.	Name of the ligand	Molecular weight (g/mol)	Lipinski Rule
1.	Chlorpromazine 	318.86	HBD= 0 HBA= 1 LogP= 4.35
2.	Thioridazine 	370.57	HBD= 0 HBA= 1 LogP= 5.03
3.	Verapamil 	454.6	HBD= 0 HBA= 6 LogP= 2.96

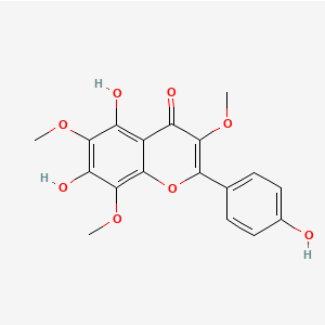
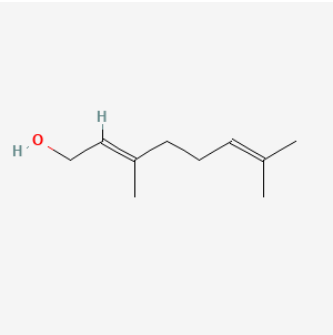
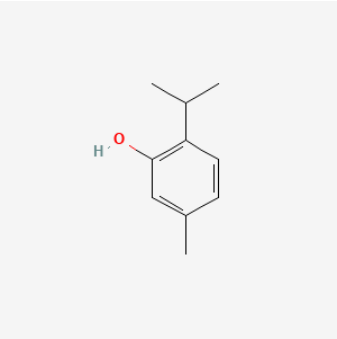
4.	CCCP 	204.62	HBD= 1 HBA= 3 LogP= 0.92
5.	DNP 	184.11	HBD= 1 HBA= 5 LogP= -0.72
6.	Reserpine 	608.68	HBD= 1 HBA= 10 LogP= 1.75

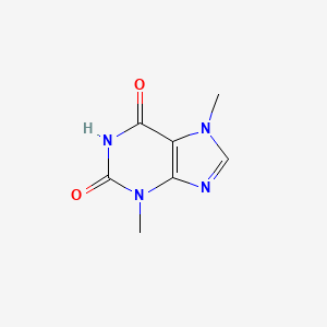
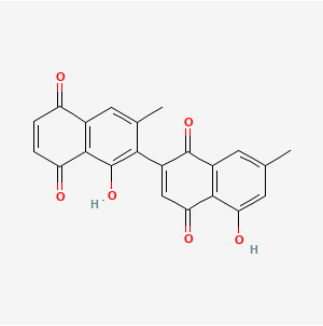
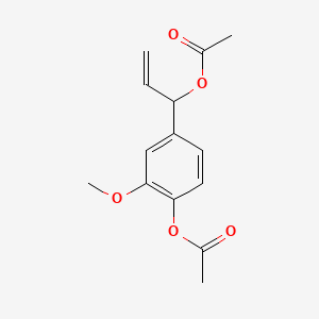
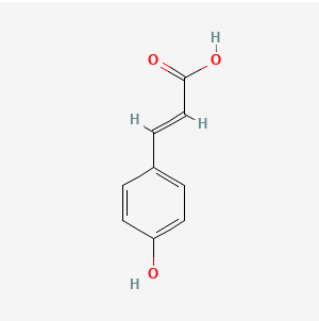
7.	Piperine 	285.34	HBD= 0 HBA= 3 LogP= 2.39
8.	Farnesol 	222.37	HBD= 1 HBA= 1 LogP= 2.39
9.	Biochanin A 	284.26	HBD= 2 HBA= 5 LogP= 0.77

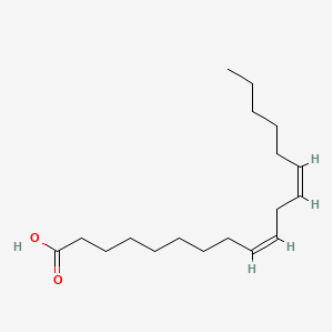
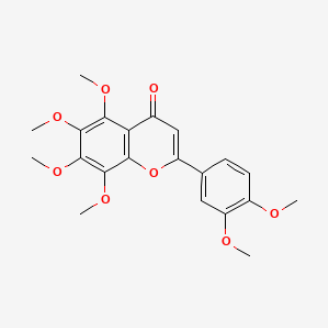
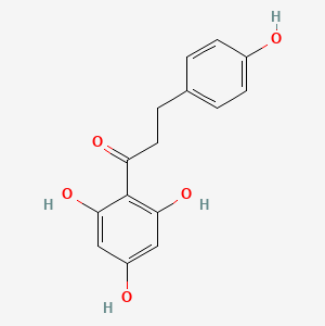
10.	Luteolin 	286.24	HBD= 4 HBA= 6 LogP= -0.03
11.	Berberine 	336.36	HBD= 0 HBA= 4 LogP= 2.19
12.	Silybin 	482.44	HBD= 5 HBA= 10 LogP= -0.4
13.	Curcumin 	368.38	HBD= 2 HBA= 6 LogP= 1.47

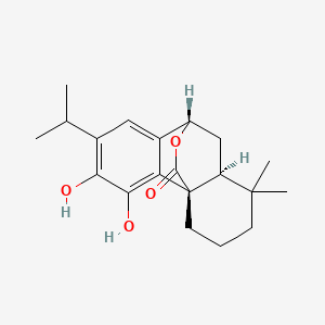
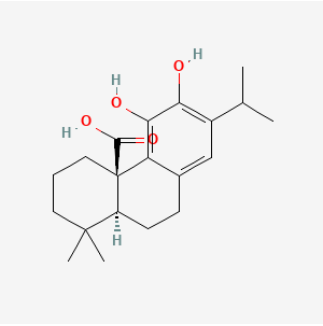
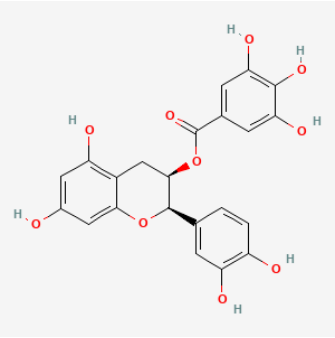
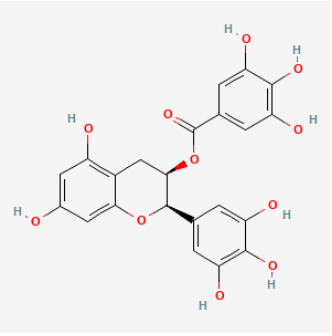
14.	Omeprazol 	713.12	HBD= 0 HBA= 12 LogP= 0.89
15.	Jatrorrhizine 	338.38	HBD= 1 HBA= 4 LogP= 1.78
16.	Columbamine 	338.38	HBD= 1 HBA= 4 LogP= 1.78

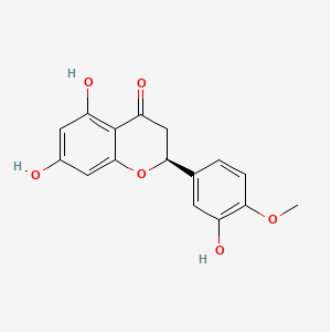
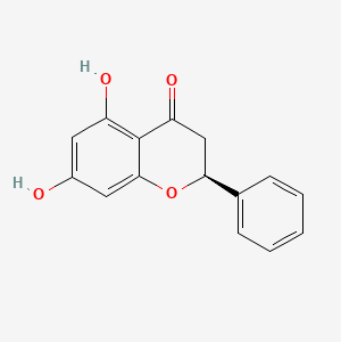
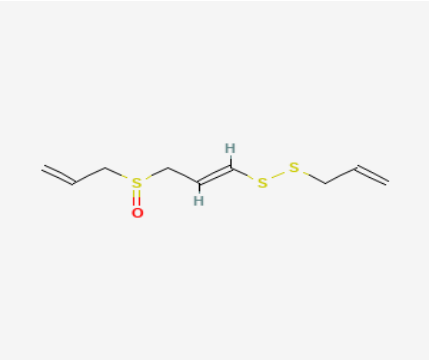
17.	Catharanthine 	336.43	HBD= 1 HBA= 3 LogP= 2.96
18.	Conessine 	356.59	HBD= 0 HBA= 2 LogP= 4.8
19.	Genistein 	270.24	HBD= 3 HBA= 5 LogP= 0.52
20.	Palmatine 	352.4	HBD= 0 HBA= 4 LogP= 2.01

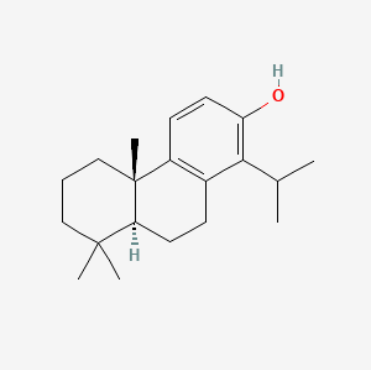
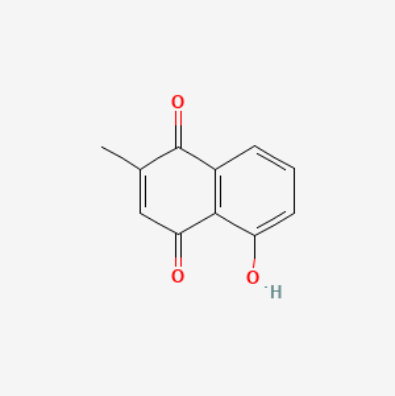
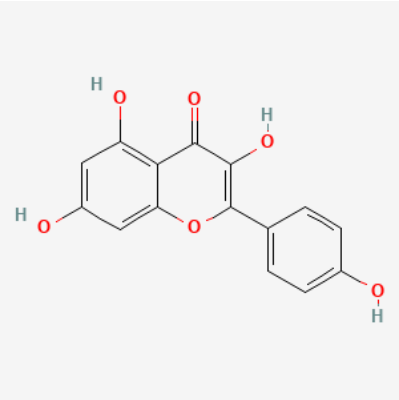
21.	Sarothrin 	360.31	HBD= 3 HBA= 8 LogP= -0.35
22.	Geraniol 	154.25	HBD= 1 HBA= 1 LogP= 2.59
23.	Thymol 	150.22	HBD= 1 HBA= 1 LogP= 2.76

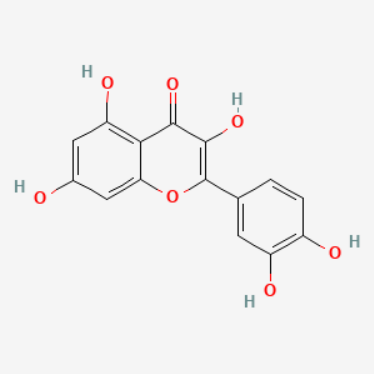
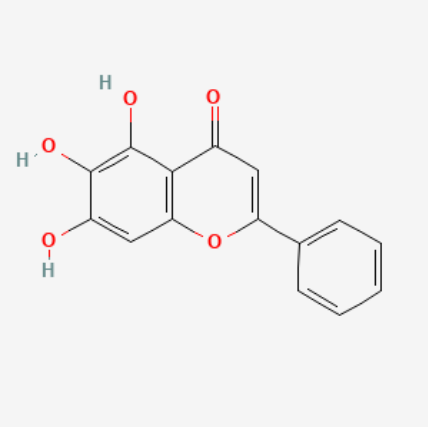
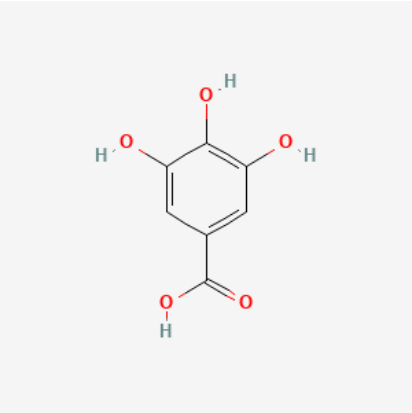
24.	Theobromine 	180.16	HBD= 1 HBA= 3 LogP= -0.12
25.	Diospyrin 	374.34	HBD= 2 HBA= 6 LogP= 0.62
26.	Phenylpropanoids (1′-S-1′-acetoxyeugenol acetate) 	264.27	HBD= 0 HBA= 5 LogP= 2.01
27.	P-coumaric acid 	164.16	HBD= 2 HBA= 3 LogP= 1.28

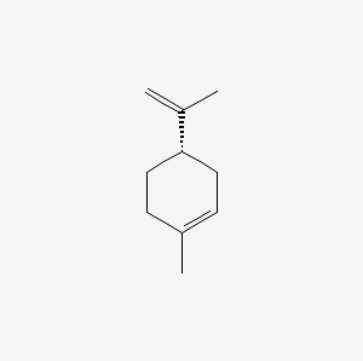
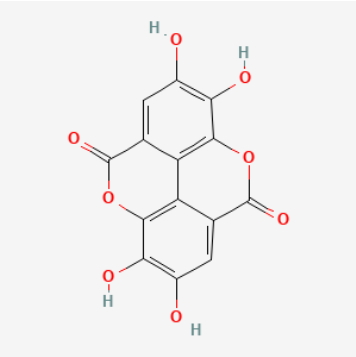
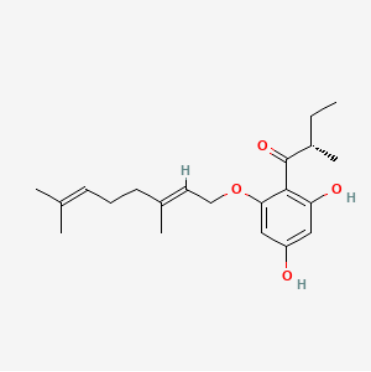
28.	Linoleic acid 	280.45	HBD= 1 HBA= 2 LogP= 1.28
29.	Nobiletin 	402.39	HBD= 0 HBA= 8 LogP= 0.34
30	Phloretin 	274.27	HBD= 4 HBA= 5 LogP= 1.1

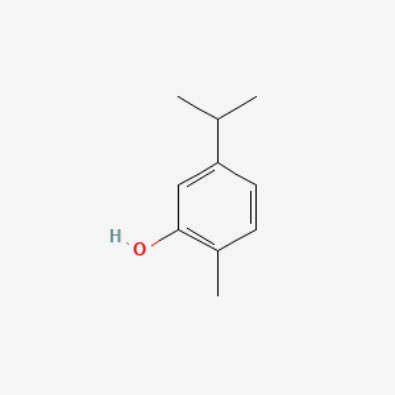
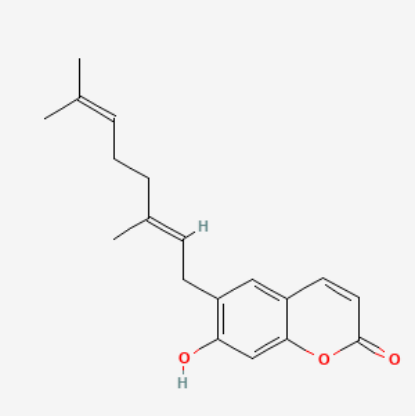
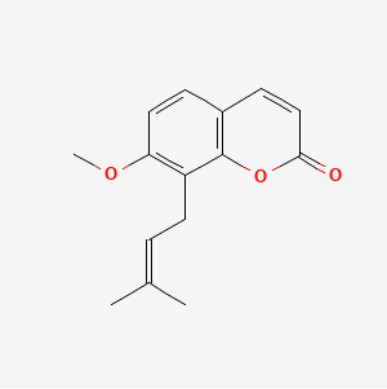
31.	Carnosol 	330.42	HBD= 2 HBA= 4 LogP= 3.25
32.	carnosic acid 	332.43	HBD= 3 HBA= 4 LogP= 3.25
33.	Epicatechin gallate 	460.52	HBD= 7 HBA= 10 LogP= -1.32
34.	Epigallocatechin gallate 	458.37	HBD= 8 HBA= 11 LogP= -0.44

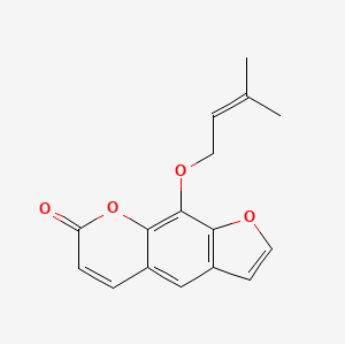
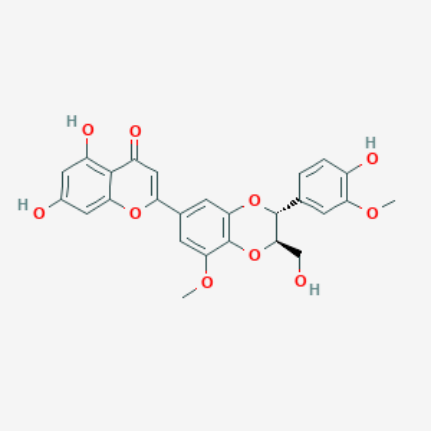
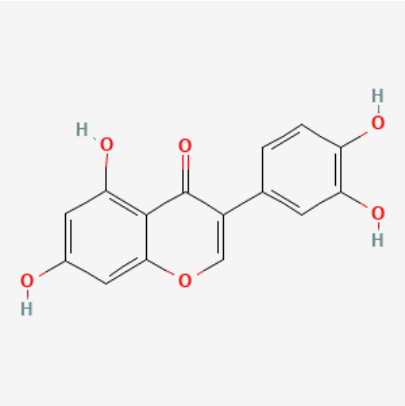
35.	Hesperetin 	302.28	HBD= 3 HBA= 6 LogP= 0.41
36.	Pinocembrin 	256.25	HBD= 2 HBA= 6 LogP= 1.27
37.	Ajoene 	234.4	HBD= 0 HBA= 1 LogP= 2.1

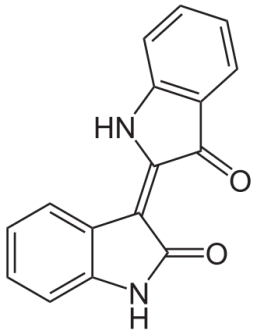
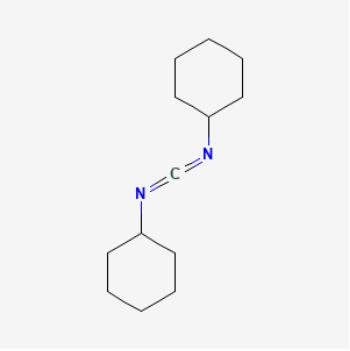
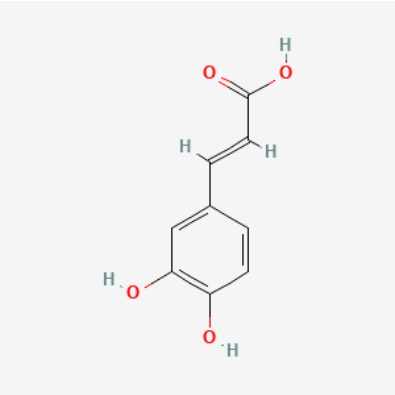
38.	Totarol 	286.45	HBD= 1 HBA= 1 LogP= 4.92
39.	Plumbagin 	188.18	HBD= 1 HBA= 3 LogP= 0.59
40.	Kaempferol 	286.24	HBD= 4 HBA= 6 LogP= -0.03

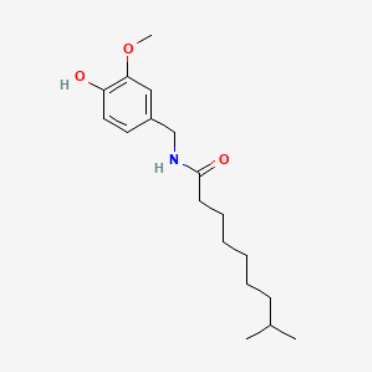
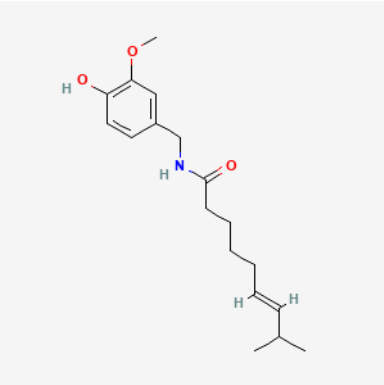
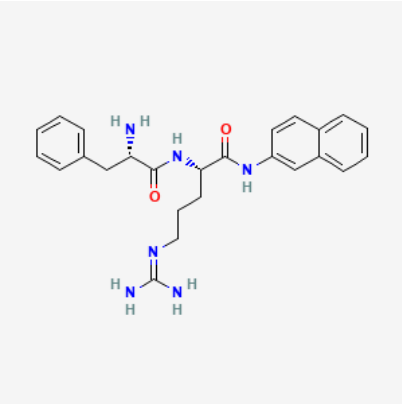
41.	Quercetin 	302.24	HBD= 5 HBA= 7 LogP= -0.56
42.	Baicalein 	270.24	HBD= 3 HBA= 5 LogP= 0.52
43.	Gallic acid 	170.12	HBD= 4 HBA= 5 LogP= -0.16

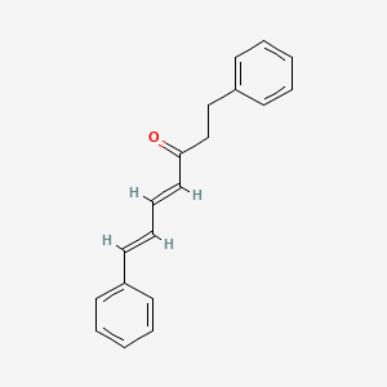
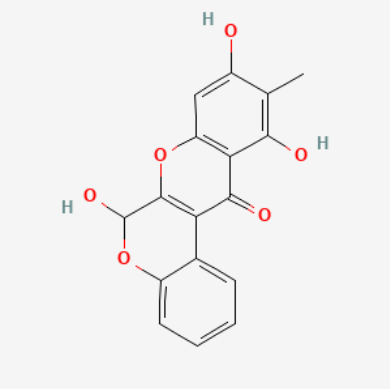
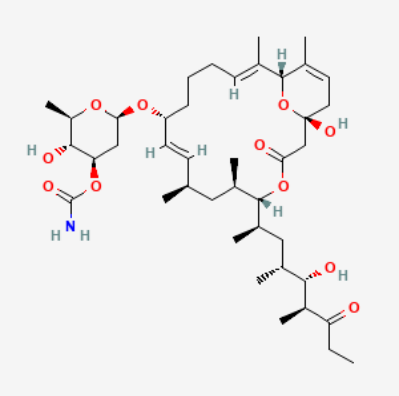
44.	Limonene 	136.23	HBD= 0 HBA= 0 LogP= 3.27
45.	Ellagic acid 	302.19	HBD= 4 HBA= 8 LogP= 0.14
46.	Olympicin A 	346.46	HBD= 2 HBA= 4 LogP= 3.16

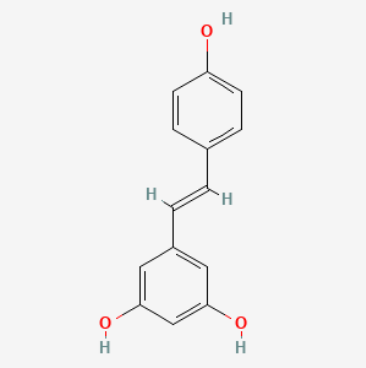
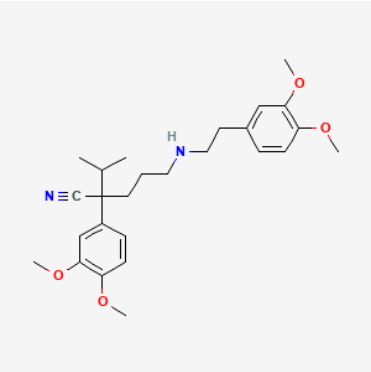
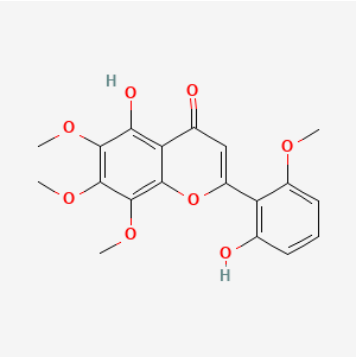
47.	Carvacrol 	150.22	HBD= 1 HBA= 1 LogP= 2.76
48.	Ostruthin (6-geranyl-7-hydroxycoumarin) 	298.38	HBD= 1 HBA= 3 LogP= 3.51
49.	Osthol 	244.29	HBD= 0 HBA= 3 LogP= 2.63

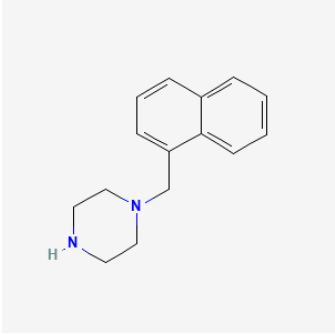
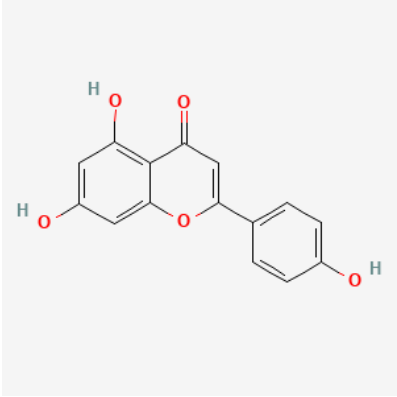
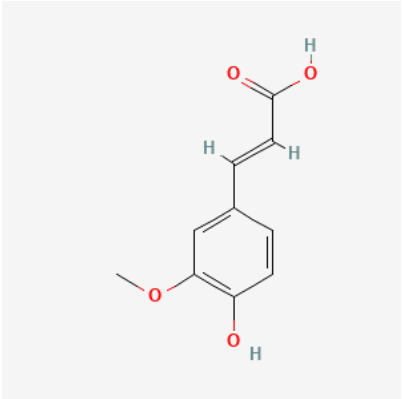
50.	Imperatorin 	270.28	HBD= 0 HBA= 4 LogP= 2.14
51.	5'-Methoxyhydnocarpin 	494.45	HBD= 4 HBA= 10 LogP= -0.1
52.	Orobol 	286.24	HBD= 4 HBA= 6 LogP= -0.03

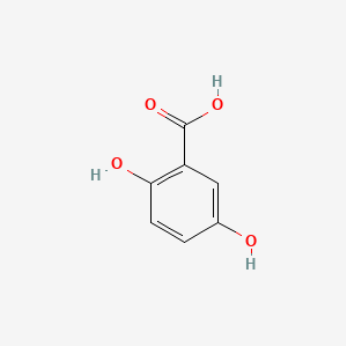
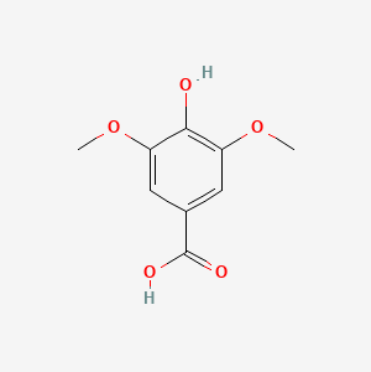
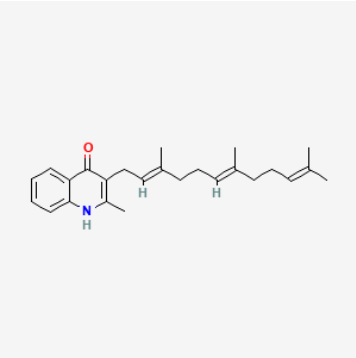
53.	Indirubin 	342.33	HBD= 3 HBA= 6 LogP= 1.01
54.	DCC (dicyclohexylcarbodiimide) 	206.33	HBD= 0 HBA= 2 LogP= 2.92
55.	Caffeic acid 	180.16	HBD= 3 HBA= 4 LogP= 0.7

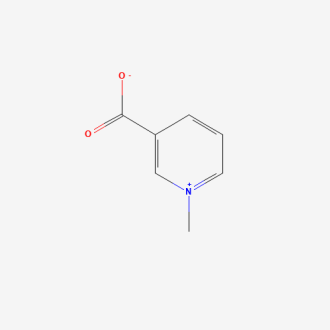
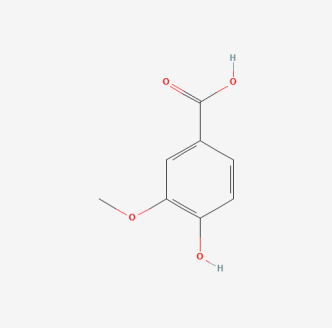
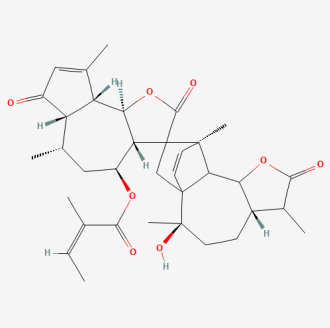
56.	Dihydrocapsaicin 	307.43	HBD= 2 HBA= 3 LogP= 2.78
57.	Capsaicin 	305.41	HBD= 2 HBA= 3 LogP= 2.69
58.	Phenyalanine-Arginine-ß-Naphthylamide 	446.54	HBD=5 HBA= 4 LogP= 1.86

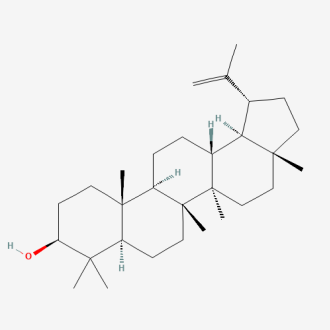
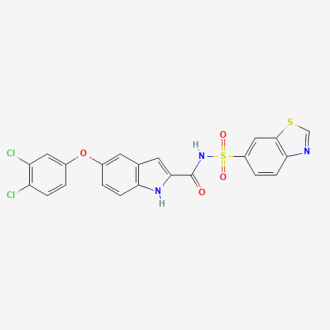
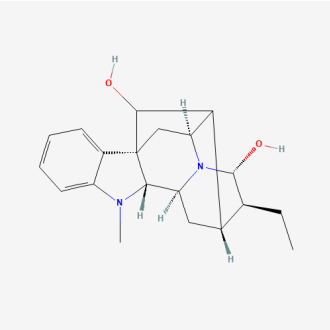
59.	Trans,trans-1,7-diphenylhepta-4,6-dien-3-one 	262.35	HBD= 0 HBA= 1 LogP= 4.33
60.	Boeravinone B 	312.27	HBD= 3 HBA= 6 LogP= 0.87
61.	Venturicidin A 	749.97	HBD= 4 HBA= 11 LogP= 2.32

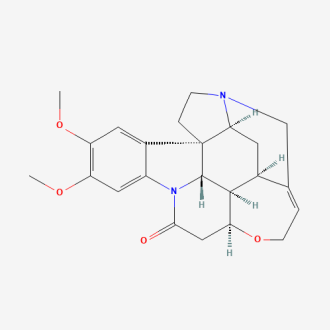
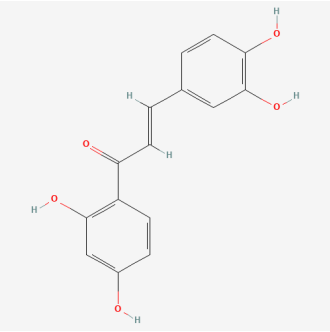
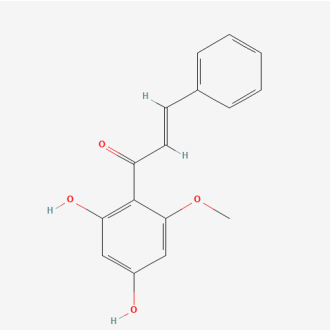
62.	Resveratrol 	228.24	HBD= 3 HBA= 3 LogP= 2.26
63.	Norverapamil 	440.58	HBD= 1 HBA= 6 LogP= 2.76
64.	Skullcapflavone II 	374.34	HBD= 2 HBA= 8 LogP= 0.12

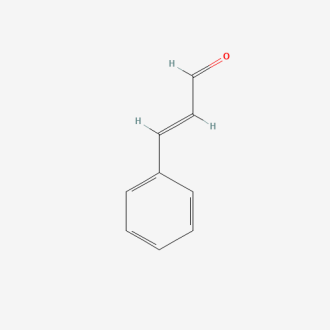
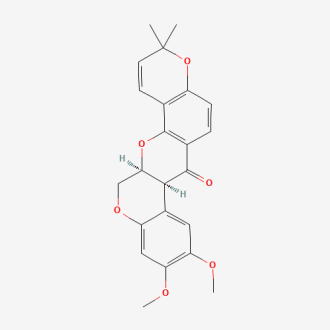
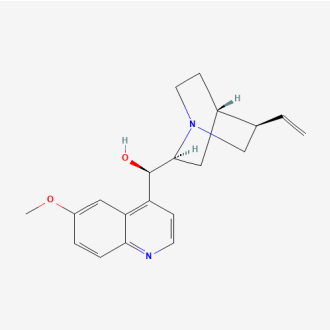
65.	NMP(1-(1-naphthylmethyl)-piperazine) 	226.32	HBD= 1 HBA= 2 LogP= 2.32
66.	Apigenin 	270.24	HBD= 3 HBA= 5 LogP= 0.52
67.	Ferulic acid 	194.18	HBD= 2 HBA= 4 LogP= 1

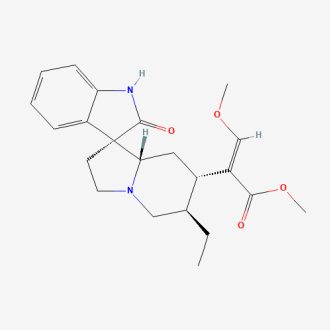
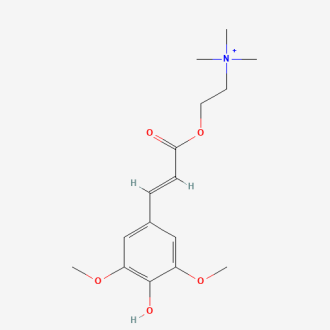
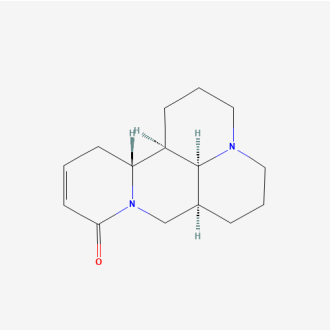
68.	Gentisic acid 	316.26	HBD= 6 HBA= 9 LogP= 1.79
69.	Syringic acid 	198.17	HBD= 2 HBA= 5 LogP= 0.49
70.	Aurachin 	404.54	HBD= 1 HBA= 2 LogP= 0.49

72.	Trigonelline 	137.14	HBD= 0 HBA= 2 LogP= 0.33
73.	Vanillic acid 	168.15	HBD= 2 HBA= 4 LogP= 0.74
74.	Arteminolide 	590.7	HBD= 1 HBA= 8 LogP= 3.78

75.	Lupeol 	426.72	HBD= 1 HBA= 1 LogP= 6.92
76.	Galectin-3 	312.32	HBD= 3 HBA= 7 LogP= -0.24
77.	Ajmaline 	326.43	HBD= 2 HBA= 3 LogP= 2.67

78.	Brucine 	394.46	HBD= 0 HBA= 5 LogP= 2.04
79.	Bulleyaconi	627.76	HBD= 1 HBA= 10 LogP= 2.04
80.	Butein 	272.25	HBD= 4 HBA= 5 LogP= 1.02
81.	Cardamonin 	270.28	HBD= 2 HBA= 4 LogP= 1.83

82.	Cinnamaldeyde 	132.16	HBD= 0 HBA= 1 LogP= 2.01
83.	Deguelin 	394.42	HBD= 0 HBA= 6 LogP= 1.93
84.	Quinine 	324.42	HBD= 1 HBA= 4 LogP= 2.23

85.	Rhynchophylline 	384.47	HBD= 1 HBA= 5 LogP= 2.02
86.	Sinapine 	310.37	HBD= 1 HBA= 5 LogP= -2.44
87.	Sophocarpine 	246.35	HBD= 0 HBA= 2 LogP= 2.16

3.3 Docking results :

The table below shows the docking results of various ligands with EfpA efflux pump.The docking was done using AutoDock4, from which the 10 best conformations were obtained. Out of these, the best 2 conformations' binding energies have been listed, which indicates good receptor-ligand binding. While multiple types of weak forces stabilize such interactions, we have considered Hydrogen bonding as the most critical.

Table 3: Showing the best two conformers in each docking with the binding energy.

S. No.	Receptor	Ligand	Run Number	Binding Energy (kcal/mol)
1	EfpA	5'-Methoxyhydnocarpin	9 7	-4.94 -4.26
2	EfpA	Ajmaline	10 8	-6.96 -6.95
3	EfpA	Apigenin	10 9	-6.40, -6.39
4	EfpA	Aurachin	3 7	-6.40 -6.31
5	EfpA	Baicalein	10 3	-6.2 -6.28
6	EfpA	Biochanin A	10 3	-6.12 -6.07
7	EfpA	Boeravinone B	3 4	-7.25 -7.24
8	EfpA	Brucine	3 8	-7.13 -7.12
9	EfpA	Butein	2 5	-5.99 -5.80
10	EfpA	Caffeic acid	8 5	-3.57 -3.53
11	EfpA	Capsaicin	7 6	-3.29 -3.21
12	EfpA	Cardamonin	2 10	-6.26 -5.69
13	EfpA	Carvacrol	3 7	-4.54 -4.50
14	EfpA	carvacrol	2 1	-3.55 -3.43
15	EfpA	Cinnamaldeyde	6 2	-4.20 -4.18
16	EfpA	Columbamine	6	-4.31

			4	-4.27
17	EfpA	Conessine	2 9	-5.11 -5.11
18	EfpA	Curcumin	5 4	-4.25 -3.87
19	EfpA	DCC (Dicyclohexylcarbodimide)	10 5	-3.85 -3.85
20	EfpA	Deguelin	3 10	-8.19 -8.19
21	EfpA	Dihydrocapsaicin	4 5	-3.95 -3.19
22	EfpA	Diospyrin	9 7	-8.50 -8.49
23	EfpA	DNP	6 10	-5.58 -5.47
24	EfpA	Ellagic acid		-9.40 -8.80
25	EfpA	Epicatechin gallate	8 2	-9.40 -7.51
26	EfpA	Epigallocatechin gallate	1 4	-8.26 -7.60
27	EfpA	Evodine		-4.15 -4.14
28	EfpA	Farnesol	4 1	-4.72 -4.57
29	EfpA	Ferulic acid	9 5	-5.10 -5.09
30	EfpA	Galectin	1 7	-5.71 -5.52
31	EfpA	Gallic acid		-6.00 -5.50
32	EfpA	Genistein	7 2	-3.77 -3.75
33	EfpA	Genistein		-2.98

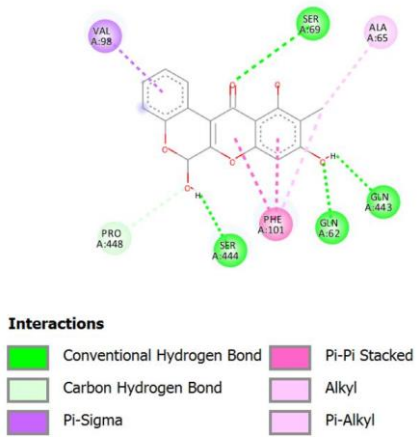
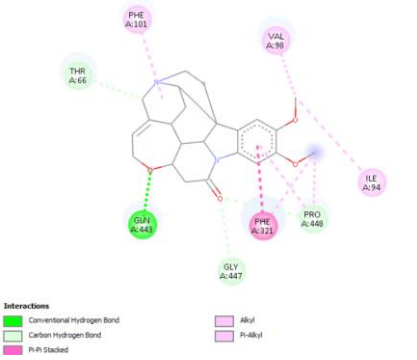
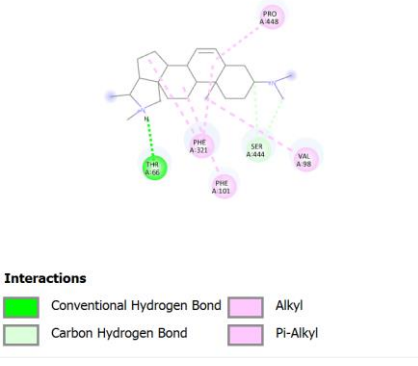
				-2.95
34	EfpA	Gentisic acid	3 2	-4.76 -4.59
35	EfpA	Geraniol	3 9	-3.79 -3.78
36	EfpA	Gelsemine		-8.81 -8.81
37	EfpA	Hesperetin	8 5	-7.58 -7.47
38	EfpA	Imperatorin	6 2	-6.10 -6.08
39	EfpA	Indirubin	10 9	-5.65 -5.49
40	EfpA	Isoniazid		-5.44, -5.41
41	EfpA	Jatrorrhizine	7 2	-4.45 -4.45
42	EfpA	Kaempferol	3 6	-8.47 -8.46
43	EfpA	Limonene		-7.10 -6.60
44	EfpA	Linoleic acid	9 2	-3.74 -3.35
45	EfpA	Loureirin		-3.43 -3.25
46	EfpA	NMP (1-(1-naphthylmethyl)-piperazine)	3 4	-5.33 -5.24
47	EfpA	Nobiletin	2 9	-7.35 -7.24
48	EfpA	Norverapamil	9 3	-5.21 -5.21
49	EfpA	Olympicin A	5 3	-5.09 -4.85
50	EfpA	Orobol	5	-3.78

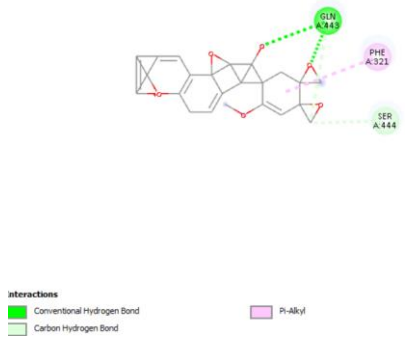
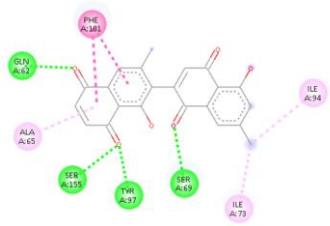
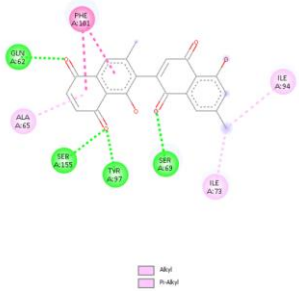
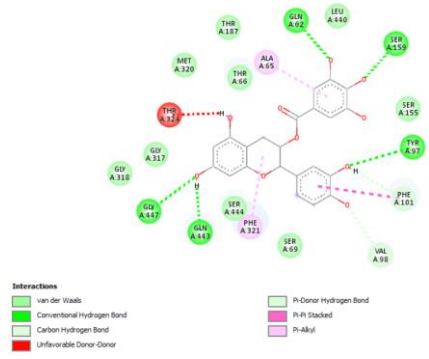
			2	-3.77
51	EfpA	Ostruthin (6-geranyl-7-hydroxycoumarin)	5 2	-6.15 -6.03
52	EfpA	Osthol	8 5	-5.76 -5.37
53	EfpA	P-coumaric acid	9 1	-4.75 -4.67
54	EfpA	Palmatine	2 3	-4.77 -4.33
55	EfpA	Phloretin	7 8	-6.14 -5.96
56	EfpA	Pinocembrin	9 5	-8.28 -8.16
57	EfpA	Piperine	9 3	-6.66 -6.65
58	EfpA	Plumbagin	5 10	-6.98 -6.97
59	EfpA	Procaine	2 8	-5.01 -4.45
60	EfpA	Protopine	8	-7.9
61	EfpA	Quercetin		-8.70 -8.20
62	EfpA	Quinine	10 7	-6.87 -6.81
63	EfpA	Reserpine	4 7	-5.88 -5.85
64	EfpA	resveratrol	9 8	-5.64 -5.60
65	EfpA	Rhynchophylline	1 8	-6.96 -6.93
66	EfpA	Sarothrin	10 3	-7.01 -6.99
67	EfpA	Sinapine	4 1	-4.02 -4.01

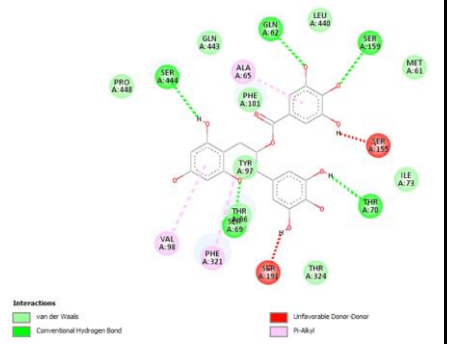
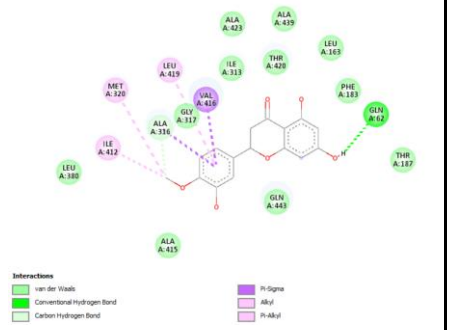
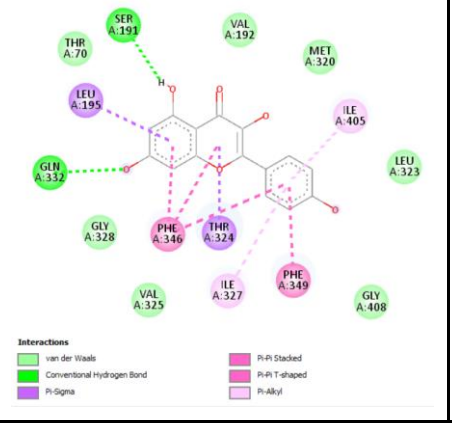
68	EfpA	Silybin	4 8	-4.49 -4.36
69	EfpA	Skullcapflavone II	7 6	-6.83 -6.81
70	EfpA	Sophocarpine	3 7	-6.10 -6.10
71	EfpA	Syringic acid	9 10	-5.10 -5.05
72	EfpA	Theobromine	8 5	-5.50 -5.49
73	EfpA	Thioridazine	2 10	-6.32 -6.04
74	EfpA	Thymol	8 5	-4.24 -4.05
75	EfpA	Trans,trans-1,7-diphenylhepta-4,6-dien-3-one	9 1	-4.64 -4.58
76	EfpA	Trigonelline	4 2	-4.33 -4.30
77	EfpA	Trovafloxacin mesylate		-2.60 -2.52
78	EfpA	Umbralisib		-3.84 -3.79
79	EfpA	Vanillic acid	9 4	-4.84 -4.84
80	EfpA	Verapamil	8 6	-5.64 -5.44
81	EfpA	Vinpocetine		-5.00 -4.58

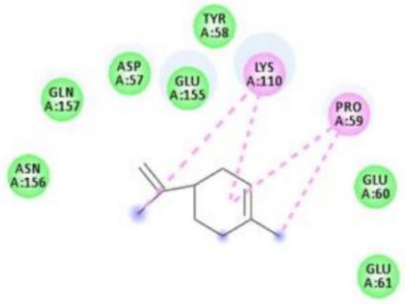
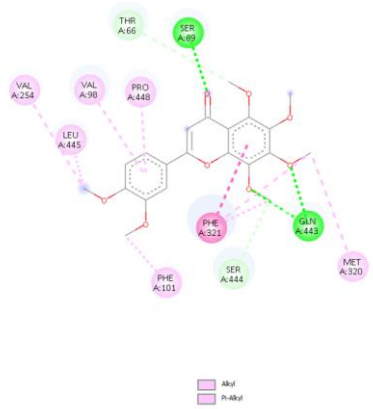
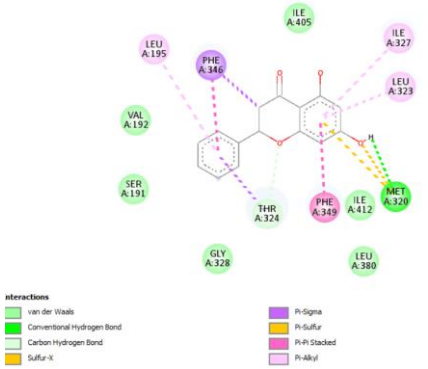
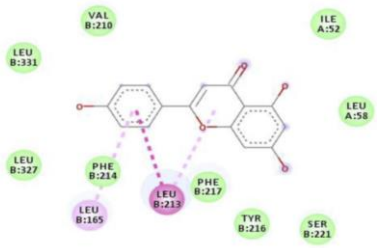
3.3 Docking Analysis

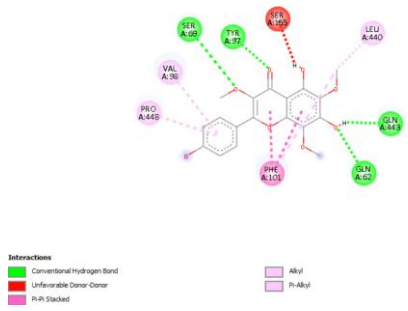
Table 4 - The following table shows the interacting residues of shortlisted ligands based on their binding energy with the active site residues of EfpA.

S No.	Name of ligand	Interacting amino acid of the protein	Hydrogen bond-forming residues	Hydrophobic interaction showing residues
1.	Boeravinone B		Q62, S69, Q443, S444	A65, V98, F101, P448
2.	Brucine		Q443, S69	V98, I94, P448, F321, M320, A65, G447, T66, F101
3.	Conessine		T66	F321,F101,S444,V98, P448

4.	Deguelin		Q443, Q62, T187	F321, V98, P448, A65, M61, L440, F101, V416, A316, Q443, L419, I313
5.	Diospyrin		Q62, S69, Y97, S155	A65, I73, I94, F101,
6.	Ellagic acid		D321, S325, S327, Y329, Q333.	
7.	Epicatechin gallate		S155, S159, Q62, I94, Q443	M61, A65, F101, T66, G447, G318, G446, P448, G317, L445, F321, S444, S69, V98, R148, I73, Y97, L440

8.	Epigallocatechin gallate		Q62, S159, T70, S69, S444	M61, L440, A65, F101, Q443, P448, Y97, I73, T324, T66
9.	Gelselmine		M105, M441, L445, S444, P448, F101	
10.	Hesperetin		Q62	T187, Q443, G317, V416, A316, I412, M320, L380, F183, L163, A423, A439, T420, I313, L419, A415
11.	Kaempferol		S191, Q332	I405, L323, G408, F349, I327, T324, P346, V325, G328, L195, T70, S191, V192, M320

12.	Limonene		I89, L93, F97, V100, L104, I201, F205, L208	
13.	Nobiletin		Q62, S69, T420, Q443	T66, V98, F101, L163, F183, A184, T187, A188, V254, I313, M320, F321, F349, M353, V416, L419, A423, A439 L440, Q443, S444, L445 ,P448
14.	Pinocembrin		G328	L195, F346, V192, S191, T324, I327, I405, P349, M320, L323, G408, L380, I412, A188
15.	Quercetin		S190, T197, N244, D321, S325, S327, Y329, Q333.	

16.	**Sarothrin**		Q62, S69, Y97, Q443	V98, F101, S155, F321, L440, P448

Results and Discussion

Site-specific docking of the selected small-molecule candidates into the defined binding cavity of MtEfpA revealed a consistent and well-resolved pattern of interactions. By restricting the docking grid to the central hydrophilic pocket—formed by TM1, TM4, TM2a, TM13, TM5, and the head groups of PEB and PEC—the analysis ensured that all ligands were evaluated directly within the functional region most likely responsible for substrate recognition and inhibitor binding. The pocket, measuring approximately 6–10 Å in width and characterized by a negatively charged interior, facilitated stable ligand orientation and reproducible docking poses across the tested compounds.

Key residues within the cavity, including Y97, S155, S69, T66, Q62, S191, Q443, and S444, were frequently involved in hydrogen bonding, electrostatic interactions, and polar contacts. Y97, a highly conserved residue oriented toward the periplasm, consistently emerged as a critical interaction partner, further highlighting its likely importance in ligand stabilization. Comparative assessment of binding affinities, interaction networks, and pocket occupancy allowed for ranking the molecules based on their predicted inhibitory strength. Several compounds displayed particularly favorable docking scores and extensive engagement with essential cavity residues, suggesting strong potential as EfpA inhibitors.

Overall, the site-specific docking approach provided a focused and structurally informed evaluation of inhibitor binding within MtEfpA. While the computational findings offer clear support for the identified pocket as a viable inhibitory site and highlight several promising lead molecules, experimental validation is still pending. Biochemical assays, efflux inhibition studies, and microbiological evaluations will be essential to confirm the predicted interactions and establish true inhibitory efficacy. These results therefore serve as a robust computational foundation for subsequent experimental investigation.

References

[1] Cohen, A. et al. (2019). The global prevalence of latent tuberculosis: a systematic review and meta-analysis of LTBI prevalence surveys. European Respiratory Journal, 54(3)

[2] Houben, R. M. G. J., & Dodd, P. J. (2016). The global burden of latent tuberculosis infection: a re-estimation using mathematical modelling. PLOS Medicine, 13(10): e1002152.

[3] Smith, I. (2003). Mycobacterium tuberculosis Pathogenesis and Molecular Determinants of Virulence. *Clinical Microbiology Reviews*, *16*(3), 463–496. https://doi.org/10.1128/CMR.16.3.463-496.2003

[4] Miggiano, R., Rizzi, M., & Ferraris, D. M. (2020). Mycobacterium tuberculosis Pathogenesis, Infection Prevention and Treatment. *Pathogens*, *9*(5), 385. https://doi.org/10.3390/pathogens9050385

[5] Warner, D. F., Barczak, A. K., Gutierrez, M. G., & Mizrahi, V. (2025). Mycobacterium tuberculosis biology, pathogenicity, and interaction with the host. *Nature Reviews. Microbiology*, *23*(12), 788–804. https://doi.org/10.1038/s41579-025-01201-x

[6] Aguilar-Ayala, D. A., Palomino, J. C., Vandamme, P., Martin, A., & Gonzalez-y-Merchand, J. A. (2017). "Genetic regulation of *Mycobacterium tuberculosis* in a lipid-rich environment." *Infection, Genetics and Evolution*, *55*, 392–402. https://doi.org/10.1016/j.meegid.2016.10.015

[7] Lawn SD, Zumla Al. Tuberculosis. Lancet. 2011;378(9785):57-72.

[8] Furin J, Cox H, Pai M. Tuberculosis. Lancet. 2019;393(10181):1642-1656.

[9] Golden MP, Vikram HR. Extrapulmonary tuberculosis: an overview. Am Fam Physician. 2005;72(9):1761-1768.

[10] Velayutham B, Nair D, Tripathy JP, Chadha SS. Clinical presentation of tuberculosis: a tertiary care experience. Int J Res Med Sci. 2017;5 (3):1075-1080.

[11] Grzegorzewicz, A. E., De Sousa-d'Auria, C., McNeil, M. R., Huc-Claustre, E., Jones, V., Petit, C., Angala, S. K., Zemanová, J., Wang, Q., Belardinelli, J. M., Gao, Q., Ishizaki, Y., Mikušová, K., Brennan, P. J., Ronning, D. R., Chami, M., Houssin, C., & Jackson, M. (2016). Assembling of the Mycobacterium tuberculosis Cell Wall Core. *Journal of Biological Chemistry*, *291*(36), 18867–18879. https://doi.org/10.1074/jbc.M116.739227

[12] Singh, P., Rameshwaram, N. R., Ghosh, S., & Mukhopadhyay, S. (2018). Cell Envelope Lipids in the Pathophysiology of *Mycobacterium Tuberculosis*. *Future Microbiology*, *13*(6), 689–710. https://doi.org/10.2217/fmb-2017-0135

[13] Singh, G., Kumar, A., Maan, P., & Kaur, J. (2017). Cell Wall Associated Factors of Mycobacterium tuberculosis as Major Virulence Determinants: Current Perspectives in Drugs Discovery and Design. *Current Drug Targets*, *18*(16). https://doi.org/10.2174/1389450118666170711150034

[14] *Global Tuberculosis Report 2023* (1st ed). (2023). World Health Organization.

[15] Zumla, A., Nahid, P., & Cole, S. T. (2013). Advances in the development of new tuberculosis drugs and treatment regimens. *Nature Reviews Drug Discovery*, *12*(5), 388–404. https://doi.org/10.1038/nrd4001

[16] Rawat, R., Whitty, A., & Tonge, P. J. (2003). The isoniazid-NAD adduct is a slow, tight-binding inhibitor of InhA, the *Mycobacterium tuberculosis* enoyl reductase: Adduct affinity and drug resistance. *Proceedings of the National Academy of Sciences*, *100*(24), 13881–13886. https://doi.org/10.1073/pnas.2235848100

[17] Marrakchi, H., Lanéelle, M.-A., & Daffé, M. (2014). Mycolic Acids: Structures, Biosynthesis, and Beyond. *Chemistry & Biology*, *21*(1), 67–85. https://doi.org/10.1016/j.chembiol.2013.11.011

[18] Zhang, Y., & Mitchison, D. (2003). The curious characteristics of pyrazinamide: A review. *The International Journal of Tuberculosis and Lung Disease: The Official Journal of the International Union Against Tuberculosis and Lung Disease*, *7*(1), 6–21.

[19] Goude, R., Amin, A. G., Chatterjee, D., & Parish, T. (2009). The Arabinosyltransferase EmbC Is Inhibited by Ethambutol in *Mycobacterium tuberculosis*. *Antimicrobial Agents and Chemotherapy*, *53*(10), 4138–4146. https://doi.org/10.1128/AAC.00162-09

[20] Webber, M. A., & Piddock, L. J. (2003). The importance of efflux pumps in bacterial antibiotic resistance. The Journal of antimicrobial chemotherapy, 51(1), 9–11. https://doi.org/10.1093/jac/dkg050

[21] Gaurav, A., Bakht, P., Saini, M., Pandey, S., & Pathania, R. (2023). Role of bacterial efflux pumps in antibiotic resistance, virulence, and strategies to discover novel efflux pump inhibitors. Microbiology (Reading, England), 169(5), 001333. https://doi.org/10.1099/mic.0.001333

[22] Rodrigues, L., Cravo, P., & Viveiros, M. (2020). Efflux pump inhibitors as a promising adjunct therapy against drug resistant tuberculosis: a new strategy to revisit mycobacterial targets and repurpose old drugs. *Expert review of anti-infective therapy*, *18*(8), 741–757. https://doi.org/10.1080/14787210.2020.1760845

[23] Piddock L. J. (2006). Multidrug-resistance efflux pumps - not just for resistance. Nature reviews. Microbiology, 4(8), 629–636. https://doi.org/10.1038/nrmicro1464

[24] Li, D., Zhang, X., Yao, Y., Sun, X., Sun, J., Ma, X., Yuan, K., Bai, G., Pang, X., Hua, R., Guo, T., Mi, Y., Wu, L., Zhang, J., Wu, Y., Liu, Y., Wang, P., Wong, C. C. L., Chen, X. W., Xiao, H., … Gao, F. (2024).

Structure and function of Mycobacterium tuberculosis EfpA as a lipid transporter and its inhibition by BRD-8000.3. Proceedings of the National Academy of Sciences of the United States of America, 121(44), e2412653121. https://doi.org/10.1073/pnas.2412653121

[25] Machado, D., Couto, I., Perdigão, J., Rodrigues, L., Portugal, I., Baptista, P., Veigas, B., Amaral, L., & Viveiros, M. (2012). Contribution of efflux to the emergence of isoniazid and multidrug resistance in Mycobacterium tuberculosis. PloS one, 7(4), e34538. https://doi.org/10.1371/journal.pone.0034538

[26] Sassetti, C. M., Boyd, D. H., & Rubin, E. J. (2003). Genes required for mycobacterial growth defined by high density mutagenesis. Molecular microbiology, 48(1), 77–84. https://doi.org/10.1046/j.1365-2958.2003.03425.x

[27] Griffin, J. E., Gawronski, J. D., Dejesus, M. A., Ioerger, T. R., Akerley, B. J., & Sassetti, C. M. (2011). High-resolution phenotypic profiling defines genes essential for mycobacterial growth and cholesterol catabolism. PLoS pathogens, 7(9), e1002251. https://doi.org/10.1371/journal.ppat.1002251

[28] Wang, S., Wang, K., Song, K., Lai, Z. W., Li, P., Li, D., Sun, Y., Mei, Y., Xu, C., & Liao, M. (2024). Structures of the Mycobacterium tuberculosis efflux pump EfpA reveal the mechanisms of transport and inhibition. Nature communications, 15(1), 7710. https://doi.org/10.1038/s41467-024-51948-9

[29] Pravda, L., Sehnal, D., Toušek, D., Navrátilová, V., Bazgier, V., Berka, K., Svobodová Vareková, R., Koca, J., & Otyepka, M. (2018). MOLEonline: a web-based tool for analyzing channels, tunnels and pores (2018 update). Nucleic acids research, 46(W1), W368–W373. https://doi.org/10.1093/nar/gky309

[30] Johnson, E. O., LaVerriere, E., Office, E., Stanley, M., Meyer, E., Kawate, T., Gomez, J. E., Audette, R. E., Bandyopadhyay, N., Betancourt, N., Delano, K., Da Silva, I., Davis, J., Gallo, C., Gardner, M., Golas, A. J., Guinn, K. M., Kennedy, S., Korn, R., McConnell, J. A., … Hung, D. T. (2019). Large-scale chemical-genetics yields new M. tuberculosis inhibitor classes. Nature, 571(7763), 72–78. https://doi.org/10.1038/s41586-019-1315-z

[31.] Hamada Y, Getahun H, Tadesse BT, Ford N. HIV-associated tuberculosis. Int J STD AIDS. 2021 Aug;32(9):780-790. doi: 10.1177/0956462421992257. Epub 2021 Feb 20. PMID: 33612015; PMCID: PMC8236666.

[32.] TB/COVID-19 Global Study Group. Tuberculosis and COVID-19 co-infection: description of the global cohort. Eur Respir J. 2022 Mar 24;59 (3):2102538.

UTILISATION CERTIFICATE

Amount sanctioned for Grant SVPG2505 =	Rs 20,000/-
Amount Utilized: 1. Invoice No.: 2025350 dated 14 Feb 2026 =	Rs 14986/-
2. Invoice no. 25-26/CS/0669 dated 10 Oct 2025 =	Rs 4998/-
Total Amount Utilized =	**Rs 19984/-**



Signature of PI

Bioport
Innovate with confidence

Retail Invoice

No.: 2025350

Date of Invoice: 14-Feb-26

Quotation Reference: 15184571

From

Bioport Solutions Private Limited
Plot No 2,3, Khasra No. 570/1/2, Nr Metro Pillar No 544, Mundka, Delhi-110041
GSTIN-07AAGCB4330F1Z2
PAN Number-AAGCB4330F
Phone: +91-8468905343
E-mail: info@bioportsolutions.com
Website: www.bioportsolutions.com

To

The Principal (SVC)

Sri Venkateswara College
Benito Juarez Rd, Dhaula Kuan
New Delhi - 110021
GSTIN: 07AAAGS0101D3Z0

Note:

Description Note	HSN/SAC	Qty	Unit	Rate	SGST	CGST	IGST	Amount
E0375-5G ('Ellagic Acid Dihydrate)	29322090	1	Pcs	₹ 5,700.00	9.00%	9.00%	0.00%	₹ 5,700.00
E0694-100MG ((-)-Epigallocatechin Gallate Hydrate)	29329990	1	Pcs	₹ 3,500.00	9.00%	9.00%	0.00%	₹ 3,500.00
Quartz Cuvette 1ml 2Side Clear	7017	1	Pcs	₹ 3,500.00	9.00%	9.00%	0.00%	₹ 3,500.00

For Cheque/Check Payments

Payable to BIOPORT SOLUTIONS PVT LTD and send it to:
137-R, Main road, Patparganj, Delhi - 110091

For Online Payment (NEFT or RGTS)

Bank name: ICICI BANK
Bank Account number: 629705016238
IFSC: ICIC0006297
Bank address: C-24 25, Acharya Niketan, Mayur Vihar, New Delhi, Delhi 110091, India

Total Amount	**₹ 12,700.00**
SGST	**₹ 1,143.00**
CGST	**₹ 1,143.00**
IGST	**₹ 0.00**
GST	**₹ 2,286.00**
Total	**₹ 14,986.00**
Paid	**₹ 0.00**
Round off	**₹ 0.00**
Balance Due :	**₹ 14,986.00**

Terms and Condition

Supply : Within 4-6 weeks after receipt of confirmed order.
Goods Once Sold will not be taken back.
Interest @ 18% p.a. will be charged after 30days.

CELLASOLUTIONS
THE LIFE SCIENCE RESEARCH COMPANION
GST NO. - 07AEDPV4185L1ZW

Tax Invoice

(ORIGINAL FOR RECIPIENT)

Cella Solutions
G-3/23, First Floor,
Model Town III
Delhi-110009
GSTIN/UIN: 07AEDPV4185L1ZW
State Name : Delhi, Code : 07
E-Mail : info@cellasolutions.in

Consignee (Ship to)
The Principle Sri Venkateswara College
Kind Attention: Dr Nimisha Sinha, Dhaula
Kuan New Delhi-110021, Project No. SVPG-2505
State Name : Delhi, Code : 07

Buyer (Bill to)
The Principle Sri Venkateswara College
Kind Attention: Dr Nimisha Sinha, Dhaula
Kuan New Delhi-110021, Project No. SVPG-2505
State Name : Delhi, Code : 07

Invoice No.	Dated
25-26/CS/0669	10-Oct-25
Delivery Note	Mode/Terms of Payment
	Against Delivery
Buyer's Order No.	Dated
Dispatch Doc No.	Delivery Note Date
Dispatched through	Destination
Terms of Delivery	

Sl No.	Description of Services	HSN/SAC	GST Rate	Quantity	Rate	per	Disc. %	Amount
1	**DNA Sequencing Value Read Pass**	998111	18 %	12.000 No.	353.00	No.		4,236.00
	Output CGST @ 9%					9 %		381.24
	Output SGST @ 9%					9 %		381.24
	Less : *Round Off*							(-)0.48
	Total			12.000 No.				₹ 4,998.00

E. & O.E

Amount Chargeable (in words)
Indian Rupees Four Thousand Nine Hundred Ninety Eight Only

HSN/SAC	Taxable Value	CGST Rate	CGST Amount	SGST/UTGST Rate	SGST/UTGST Amount	Total Tax Amount
998111	4,236.00	9%	381.24	9%	381.24	762.48
Total	4,236.00		381.24		381.24	762.48

Tax Amount (in words) : **Indian Rupees Seven Hundred Sixty Two and Forty Eight paise Only**
Company's PAN : **AEDPV4185L**

Declaration
We declare that this invoice shows the actual price of the goods described and that all particulars are true and correct.

Company's Bank Details
Bank Name : **ICICI BANK (OD C/A 1st)**
A/c No. : **016005006880**
Branch & IFS Code: **Model Town III & ICIC0000160**

Customer's Seal and Signature

for Cella Solutions

This is a Computer Generated Invoice